sustainability

MDPI

Article

The Visual Greenery Field: Representing the Urban Green Visual Continuum with Street View Image Analysis

Gabriele Stancato

Department of Architecture and Urban Studies, Politecnico di Milano, 20133 Milan, Italy; gabriele.stancato@polimi.it

Abstract: This study proposes a method to analyze urban greenery perceived from street-level viewpoints by combining geographic information systems (GIS) with image segmentation. GIS was utilized for a geospatial statistical analysis to examine anisotropy in the distribution of urban greenery and to spatialize image segmentation data. The result was the Visual Greenery Field (VGF) model, which offers a vector-based representation of greenery visibility and directionality in urban environments. The analysis employed street view images from selected geographic locations to calculate a Green View Index (GVI) and derive visual vectors. Validation confirmed the reliability of the methods, as evidenced by solid correlations between automatic and manual segmentations. The findings indicated that greenery visibility varies across the cardinal directions, highlighting that the GVI's average value may obscure significant differences in greenery's distribution. The VGF model complements the GVI by revealing directional coherence in urban greenery experiences. This study emphasizes that while the GVI provides an overall assessment, integrating the VGF model enriches the understanding of perceptions of urban greenery by capturing its complexities and nuances.

Keywords: green view index; street view image; semantic segmentation; urban forestry; visual greenery field

Citation: Stancato, G. The Visual Greenery Field: Representing the Urban Green Visual Continuum with Street View Image Analysis. *Sustainability* **2024**, *16*, 9512. https://doi.org/10.3390/su16219512

Academic Editor: Tommaso Caloiero

Received: 30 August 2024
Revised: 16 October 2024
Accepted: 29 October 2024
Published: 31 October 2024

1. Introduction

The United Nations' Goal 11 (Sustainable Development Goals) suggests the development of inclusive, safe, resilient, and sustainable cities; in particular, Goal 11.7 stresses the need for safe and accessible green and public spaces by 2030 [1]. While accessibility should be primarily physical, this concept can be linked to visual continuity and permeability [2–5] as components of exposure to greenery [6]. In addition, the amount and distribution of green spaces can affect urban safety and crime prevention [7,8]. For this reason, identifying the predominant direction from which urban greenery is perceived can be relevant to assessing how accessible and usable greenery is for citizens in terms of physical interaction and visual enjoyment [5,9–11]. In terms of the socioeconomic effects, the perception of green places is a factor that can influence housing prices [12] and weave individual needs into a social communion of space [13]. When developing a comprehensive urban planning policy, it should be considered that a significant part of urban greenery can be private, such as in Padua, where private green spaces cover up to 80% of all the urban greenery [14]; in some cases, the trend in housing development is more focused on private or semi-private green spaces at the expense of public once [15,16]. The distribution of greenery can be uneven and bland, from a high level to zero in a short range from the street crossing, generating a decay in perceptual intensity [17]. Furthermore, a public green space can be visually available from the surrounding buildings, while the only part of private vegetation that is generally visible from a public space is the vertical one (e.g., trees that rise in a yard, shrubs on the perimeter), which are typically smaller than a public garden and embedded in a built matrix [18]. Few cases consider how private vegetation can be designed to explicitly aimed at public viewing; a very famous case is the Vertical Forest of Boeri, the façade of

which appears to be completely covered in vegetation [19]. Public green spaces cannot compensate for the lack of private green spaces [20], as they have complementary functions and should be considered parts of a whole ecosystem. Landlords rarely consider their private gardens to be part of a larger environment [21], and this type of vegetation is also less visible in some towns [22] because walls hide it or it is surrounded by buildings [23]. The Green View Index (GVI) [24] is an important metric to assess urban greenery from a pedestrian's perspective, using street-level images to quantify the visibility of green spaces. Based initially on green pixel counting, nowadays, the technique for calculating GVI has been refined thanks to semantic segmentation methods; for example, Zhang [25] used deep learning models such as PSPNet to segment street view images, allowing a precise calculation of GVI based on cylindrical urban panoramas. This approach improved precision and facilitated large-scale assessments of urban greenery, as shown by studies using street view images (SVI) to analyze the spatial distribution of urban greenery [26]. One of the key gaps in the current literature is the Green View Index's limitation as an omnidirectional average value. Although several studies have investigated the correlation between the areal GVI distribution and socioeconomic or health factors [7,8,27–29], research gaps remain in identifying the directional variability of green visibility in these aspects. This leaves a gap in understanding how greenery is perceived differently from multiple viewpoints within the urban fabric, which is crucial for urban planning and development of policies aimed at improving green exposure and its positive effects. Although GVI effectively quantifies the overall visibility of greenery, it does not account for its spatial orientation; as a result, it cannot differentiate whether the same amount of greenery forms a single concentrated mass or multiple smaller patches surrounding the observer. These two scenarios, despite having identical GVI values, lead to markedly different perceptual experiences and urban spatial arrangements. Filling this gap becomes more pressing, considering the growing trends in urbanization and the need to integrate greenery into urban environments to maximize its esthetic and functional benefits. The urgency to address these gaps is underscored by the increasing awareness of green spaces to improve mental and physical health, promote social cohesion, and mitigating the effects of climate change.

Understanding the orientation of green spaces from different perspectives is useful for promoting equitable availability and supporting the creation of inclusive, resilient communities as cities expand. This work aimed to promote a focus on urban greenery as a visual congruency that involves private and public greenery from a street perspective, considering the spread and directionality of vegetation as essential factors for developing a healthy environment. The final goal was to represent the congruency and directionality of green spaces to complement the Green View Index (GVI); whereas the GVI provides a quantitative index of greenness, the proposed system provides a qualitative representation of congruency throughout the analyzed area and the visual directionality of specific locations. For this reason, this article is intended to answer the following research questions.

- Q1: How can a vector-based method quantify and represent the intensity and spatial distribution, accounting for directional visibility from street-level perspectives?
- Q2: How can urban greenery's directionality and spatial distribution be represented to visualize the coherence and intensity of green visibility across an urban environment?

2. Review of the Literature

2.1. Methodology

A scoping review was conducted, based on the Preferred Reporting Items for Systematic Reviews and Meta-Analyses (PRISMA) guidelines [30], focusing on the state of the art regarding the Green View Index over the past 10 years (2013–2023). The search queries were structured for the Scopus, Dimensions, and Web of Science databases; an extended explanation of the process can be found in Appendix A.

2.2. Use of Street View Images in Urban Greenery Assessment

Recent studies have increasingly used street view images to assess and analyze urban greenery. Biljecki and Ito [31] comprehensively reviewed how street-level images have become integral to urban analytics and GIS. This is widespread in diverse research domains, such as well-being, transportation, walkability, and socioeconomics. The origin of this concept stems from the pioneering work of Yang et al. [24], who introduced a semi-manual method to compute the amount of visible greenery by isolating green pixels from four photos shot by the researcher at each sample point, one in each cardinal direction. However, the green value was obtained by summing the green values from all four directions, giving a single overall value for each point instead of separate directional measures. Based on this, Li et al. [26] explored the automation of the Green View Index (GVI) through Google Street View™ (GSV) using spherical tiling for a complete evaluation of the surroundings. They observed that computing green elements at the street level can capture vertical vegetation and horizontal green surfaces that are not fully available to overhead remote sensing techniques. Labib et al. [32] introduced a novel approach to map eye-level greenness visibility at high spatial resolutions using multisource data, a visual decay function, and viewshed analysis. Their work emphasized that backyards and community parks usually do not contribute to the visual experience of neighborhood greenery. Ye et al. [5] integrated high-resolution GSV images with a space syntax analysis of the street network to measure the accessibility of greenery. This approach can help urban planners prioritize interventions by identifying areas with high or low access to greenery, thus informing better urban planning practices.

2.3. Advances in Green View Index Methodologies

Larkin and Hystad [27] analyzed the correlation between the normalized difference vegetation index (NDVI) and GVI, finding that they describe different aspects of the urban environment that cannot be directly derived from one another. Hua et al. [22] developed similar research and assessed that the correlation between green view factors and the NDVI is influenced by the morphology of a district, revealing that while the GVI correlates strongly with the canopy coverage near sample sites, it does not necessarily provide the same information as satellite images and vice versa.

Further refining the concept, Yu et al. [33] introduced the Floor Green View Index (FGVI), which assesses the visibility of urban vegetation from specific floors of city buildings, noting significant variability in green visibility depending on the orientation of the building. Long and Liu [34] developed an automatic method using Tencent™ Street View to assess street greenery in Chinese cities, finding that greener streets are often longer and are located in cities with higher economic production values.

Similarly, Dong and Zhang [35] calculated the GVI using the segmentation of the images of Tencent™ Street pictures on Beijing roads to analyze the relationship between the parameters of the streets' dimensions and GVI, uncovering the spatial distribution and differences in the greenery on various types of roads, confirming that the length of the road influences the GVI. Gong et al. [36] developed a method to estimate and map the sky view factor (SVF), the tree view factor (TVF), and the building view factor (BVF) in high-density Hong Kong urban environments using GSV panoramas; this approach underscored the importance of considering multiple environmental factors in complex urban landscapes. Hu et al. [37] collected LIDAR data and panoramic images throughout downtown Jinzhou City (China) and developed a method to extract the canopy line from mobile LIDAR data, identifying two basic elements, peaks and gaps, from street canopy lines and extracting six indexes (richness of peaks, evenness of peaks, frequency of peaks, total length of gaps, evenness of gaps, and frequency of gaps) to describe the fluctuations and continuities of tree canopy lines; they analyzed the abundance and spatial distribution of these indexes together with survey responses on the esthetical effects and found that most of them were significantly correlated with perceptions of vegetation on the streets. Seiferling et al. [38] used computer vision to quantify and map the distribution of urban

trees, using 90° field of view (FOV) images collected in a linear sequence in the direction of the street, providing a method for evaluating the profile of street greenery to develop a robust predictor of spatial variation in tree cover in a district using street-level pictures only. Richards and Edwards [39] used Google™ Street View (GSV) with a 90° upward pitch to measure Singapore's green canopy coverage. They identified key elements of canopy lines and highlighted that these shape indexes significantly influence the amount of visible urban greenery and sky, providing valuable information for urban planning and management.

2.4. Socioeconomic Impacts of Urban Greenery

Complementing these findings, Zhang and Dong [40] examined how visible greenery affects housing prices in Beijing, finding an increase of 10% in house prices associated with higher values of the Green View Index. Expanding the geographic scope, Li [41] studied 10 years of street view pictures to evaluate the variation in the green canopy of New York City over a long time, discovering that while the GVI values have increased slightly over time, the distribution remains uneven between neighborhoods, particularly affecting Hispanic communities, which tend to live in neighborhoods with lower GVI values.

The evolving methodologies also extend to advanced technologies. Wang et al. [42] used deep learning to assess quality in Guangzhou, linking the disparities in exposure to the socioeconomic conditions of the neighborhood and demonstrating the utility of advanced machine learning methods for measuring the economic effects of urban greenery. Street-level images have also been applied to social issues. Zhou et al. [7] used GSV images to investigate the relationship between the micro-built environment and drug-related activities, suggesting that the study of green spaces' distribution can help in reducing criminality. Their findings also indicated that less managed and more accessible areas are more prone to drug activities, suggesting the utility of street view variables in crime forecasting.

2.5. Transportation Studies and Urban Greenery

The growing role of street-level images in urban environmental research also extends to transportation studies. Ito and Biljecki [29] evaluated bikeability using street view images and computer vision. They developed a bikeability index based on automatic machine learning and computer vision methodologies that outperformed traditional methods and are scalable across different urban contexts.

Lu et al. [43] explored the relationship between urban greenness and cycling behavior in Hong Kong. The study compared two metrics of street view and eye-level greenness, finding that street greenness positively influences the likelihood of cycling. This insight suggests that improving daily exposure to greenery could promote cycling in urban environments and healthier behaviors. Similarly, Lu, Sarkar, and Xiao [44] examined the impact of street-level greenery on walking behavior in Hong Kong. They found that street greenery significantly predicts walkability and can be even more influential than parks. Their findings emphasize the importance of integrating greenery into urban design to improve walkability.

Lu [45] used GSV to investigate the association between street greenery and recreational physical activity in Hong Kong. The study revealed that the quality and quantity of vegetation are positively linked to physical activity, highlighting the role of well-designed urban greenery in promoting public health. This result was confirmed by Xiao's research [46] on elderly behavior. Ki and Lee [47] also analyzed the effects of greenery on walking time, using GSV and deep learning to calculate the GVI. Their study highlighted that GVI is more closely associated with walking behavior than traditional overhead greenness measures. This information suggests that different greenness metrics can provide varying insights into how greenery influences urban activities.

2.6. Health Implications of Urban Greenery

In the context of health research, Larkin and Hystad [27] evaluated the use of GSV to measure exposure to green spaces in health research, concluding that GSV-based metrics,

such as GVI, are valid tools for assessing exposure to green spaces. Their comparison with traditional metrics such as NDVI and tree cover showed that GSV provides complementary information, which is particularly relevant in understanding the impact of green spaces on physical and mental health. Wang et al. [8] explored perceptions of the built environment and their association with urban perception among older adults in Beijing. Using street view images and deep learning, they found that perceptions of safety, beauty, and liveliness, among other factors, are related to physical and mental health, highlighting the importance of integrating subjective perceptions into urban health research. Huang et al. [48] used panoramic image segmentation associated with automatic facial expression to verify that the higher the visible greenery, the higher the positive emotional effect, and this result occurred even in places with a low NDVI. Kang et al. [49] comprehensively reviewed how street view images are used in public health studies to sense urban environments. They discussed the strengths and challenges of using street view images to quantify urban environments, highlighting the potential of eye-level image analysis to correlate with social and sports behaviors.

Zhang, Tan, and Richards [50] investigated the relative importance of the quantitative and qualitative aspects of urban green spaces (UGS) in the promotion of health. They found that on a smaller buffer scale (100 m), visible greenness measured by GVI is more strongly associated with mental health, suggesting that fine-scale, human-centered greenness metrics may be critical to understanding the health benefits of UGS.

On a different note, Helbich et al. [28] explored the relationship between green and blue spaces and geriatric depression in Beijing, finding an inverse association between greenery and depressive symptoms. In a subsequent study, Helbich et al. [51] aimed to explore potential differences various greenness metrics and the potential influence on mental health. However, their findings did not confirm a clear relationship between the metrics and mental health outcomes. They suggested that more research is needed before favoring one greenness metric over another.

2.7. Current Trends

He and Li [52] reviewed research trends to evaluate the urban neighborhood environment using street view image processing. They categorized the research into five broad areas (thermal environment, neighborhood morphology, neighborhood environmental perception analysis, socioeconomic environment, landscape design, and environmental assessment), highlighting the growing use of street view images in urban studies, and identified key parameters and research fields derived from these images. These studies illustrate the diverse applications of street-level images in urban research, evaluating both the physical environment and the psycho-social effects to inform urban planning and design. In conclusion, while previous research has explored multidisciplinary aspects employing the Green View Index through panoramic image segmentation for measuring urban green features, these approaches often focus on areal descriptions or have limited their analysis to specific directional views such as a street axis. Currently, the use of image segmentation in urban studies is evolving to incorporate dynamic aspects such as temporal variations [41] and the integration of 3D and semantic models [32,53], capturing changes over time and adding spatial metric analyses.

This work addresses the gap by introducing a vector-based method that combines GVI with directional data, generating a Visual Greenery Field (VGF) to quantify visible greenery's intensity and orientation. This method offers a more detailed representation of urban greenery and its spatial orientation, providing a framework for analyzing green visibility within urban street networks.

3. Materials and Method

3.1. Workflow

The procedure adopted involves the following steps (Figure 1): (1) data collection, i.e., the selection of the street network's official shapefiles, street view image databases, and

semantic pre-trained CNN models; (2) data processing, i.e., generation of sample points on the street network, segmentation of the image, registration of the features' quantitative data, and validation of the semantic segmentation data; (3) data analysis, i.e., computation of the directional and average GVI values, geospatial analysis (Moran's I, variograms), and verification of the directional similarity; and (4) data representation, i.e., plots of the urban green vectors, streamplots of the visual greenery field, and comparisons with the GVI heatmap. A list of all instruments and materials adopted can be read in Appendix B.

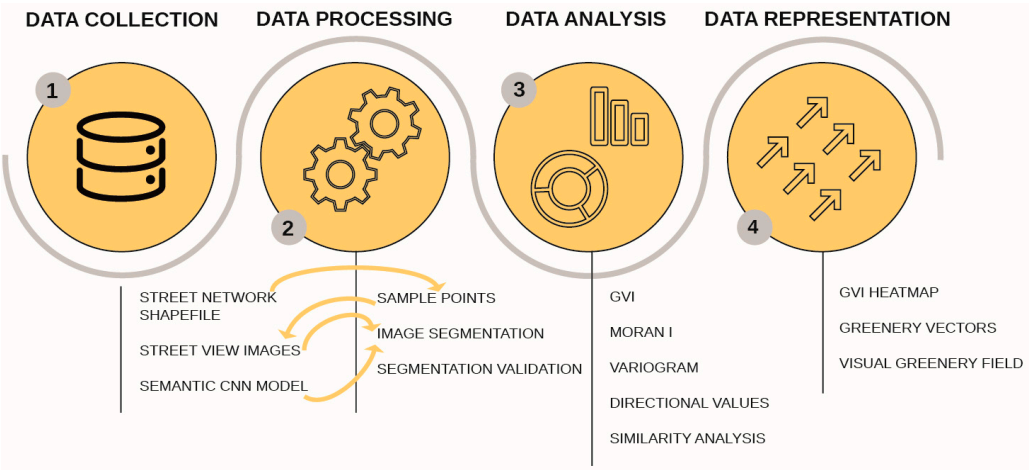

Figure 1. Research workflow. (1) Data collection: street network shapefiles, street view database, and the semantic CNN model; (2) data processing: generation of sample points, image segmentation, and validation of automated segmentation; (3) data analysis: GVI computation, Moran's I analysis, variogram analysis, analysis of significant differences in the directional values; and (4) data representation: GVI heatmap, greenery vector arrows, and streamplots of the visual greenery field.

3.2. Data Collection and Processing

The points for conducting the analyses were identified using Milan's street network provided by Milan Municipality [54]. Sample points were generated on the road grid using the "vector—random points on lines" function in QGIS, with settings of a minimum distance of one point every 50 m and a global minimum distance of 30 m. These distances allowed the placement of points even on dual carriageways while maintaining broad and adequate area coverage. The random point system was adopted to ensure a fair distribution of viewpoints in the study area, avoiding overcrowding of points near intersections where multiple roads converge. Additionally, this system avoided any pre-selected points of interest by sampling the entire area solely on a geometric basis.

To analyze the quantity of observable urban greenery while walking, driving a car, or riding a moped or bicycle, images captured by Google Street View™ were used, as they currently constitute the dataset with the broadest coverage of georeferenced spherical panoramic street images available, and are also the most up to date. For each geographic point, four images were collected from Google Street View™ with the camera oriented in the four cardinal directions (north, east, south, west) using the parameters of heading 0°, 90°, 180°, and 270°; a pitch of 0°; a field of view of 90°; and a size of 640 × 640 pixels, with a resolution of 72 DPI, which is the maximum possible size with the adopted technology. Therefore, these images coincided pairwise on the vertical sides and completed a 360° view (Figure 2). It should be noted that the Google™ API does not necessarily provide images precisely located at the coordinates sent because there is no continuous road tracking, but instead a series of georeferenced shots taken along the route [55]. Therefore, the API searches for the closest location to the requested one from those in the Google™ archive. For traceability purposes, for each Street View™ image, the corresponding file containing all metadata with the precise location of the actual point and the URL of the corresponding 360° view was also saved. From the metadata, it was verified that the images were captured

in April 2023. For each urban picture, image segmentation was performed using the GluonCV library, recording the percentage of area occupied by each detected feature. The percentages of vegetative elements present in the image were summed to obtain a synthetic value of greenery, unifying the following categories from the ADE20K model [56]: tree, plant, palm, grass, flower, and field. For each geographic point, four directional values were obtained; these values were adopted as the intensities of vectors oriented in the corresponding visual direction (north, east, south, west). The average of these four values corresponded to the Green View Index relative to a specific point in the space [26]. Therefore, the principle of vector summation was adopted to establish the synthetic green vector for a specific location. The direction of the resulting vector represents an average or weighted direction that maximizes the visibility of urban greenery, considering all four original directions. This result means that the direction of the resulting vector is the one toward which the urban greenery is most visible.

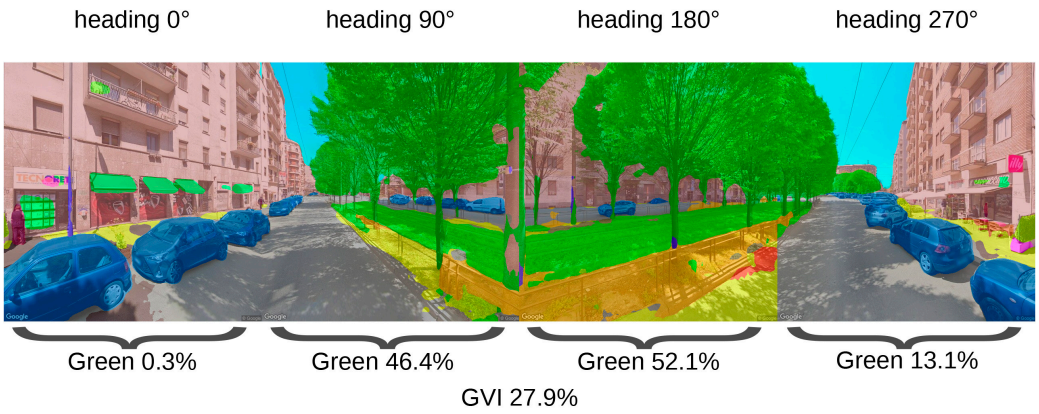

Figure 2. An example of a segmented image sequence; the camera was progressively rotated by 90°. In this overview, the colored hatches highlight different features in the scene. Source: Original image from Google Street View™, with elaboration by the author.

Since semantic segmentation is one of the most critical phases in the sequence due to its computational weight, the risk of potentially harmful interruptions in the process with consequent data loss, and the possible ambiguity in the automatic interpretation of features, it was necessary to adopt procedures to validate the outcome of segmentation. Following the segmentation process, it was verified that the number of records in the dataset corresponded to the number of images initially downloaded from Street View. It was also ensured that the number of records corresponding to each Street View point matched four images. A random sample of 100 images was randomly selected from the original dataset for data validation, and manual segmentation was performed using Adobe Photoshop™ on that subset. The vegetation areas were manually colored red, while the rest of the image was darkened with black fill. Using the OpenCV library, the percentage of red pixels was determined in the validation sample's images, and the result was compared with the automatic segmentation values. Validation was considered successful for correlation values of r-squared > 0.80 and r > 0.90, with a p-value < 0.01.

3.3. Data Analysis

Since each geographical point corresponds to four images in the respective cardinal directions, it was possible to represent the perceivable greenery of these views as the four normal vectors to the image plane with the origin at the view's vantage point location and having an intensity corresponding to the ratio of vegetation in the image. Consequently, the synthetic vector relative to the single geographical point could be obtained using a vector sum of the four previously obtained vectors. For the alignment of the geographical system with the X and Y directions of the 2D coordinate system used for the vector field computation, vectors pointing south and west are conventionally considered negative,

while vectors pointing north and east are conventionally considered positive. The direction of the resulting synthetic vector represents the direction of maximum visual exposure to the surrounding vegetation at the point of analysis:

$$\text{Visual Greenery Vector}\left(\vec{v}\right) = \vec{N} - \vec{S} + \vec{E} - \vec{W}.$$

To evaluate whether the differences in greenery values between pairs of cardinal directions were significantly distinct, the differences between all possible pairs of directions (e.g., north–south, east–west, north–East, and south–west) were calculated. By evaluating these differences, it was possible to determine whether the distribution of visible greenery was uniform or varied significantly depending on the viewing direction. If the phenomenon remained consistent, the differences between pairs should be statistically similar, indicating that the green visibility was evenly distributed in all directions. A Friedman test was then performed on these differences to assess whether the variance between the pairs of directions was statistically significant. Following the Friedman test's results, Dunn's test was conducted to further investigate the specific pairs of cardinal directions that exhibited significant differences in the distribution of greenery. This approach allowed for a detailed examination of the directional disparities in the visibility of urban vegetation.

To verify the visual vector representation model, 50 new random points were generated in QGIS on the Città Studi district road network. For each new point, the four images were extracted in the cardinal directions, and then image segmentation and GVI calculations were performed. Subsequently, the visual vector was calculated for the new set of images. For the validation of the vectors' values and their representativeness, the intensity of each vector in the original dataset was compared with the nearest vector from the validation set. For each pair of vectors, the following information was collected in a dataframe: the alphanumeric identifiers of the vectors' anchor point, the geodesic distance between the pairs of points, and the vectors' magnitude

$$\|v\| = \sqrt{v_x^2 + v_y^2};\ \|u\| = \sqrt{u_x^2 + u_y^2}$$

where u and v are the normalized vectors of the original and the validation datasets, and $||v||$ and $||u||$ are the magnitudes of the vectors. The new dataframe was filtered to exclude all point pairs with distances less than 1m and greater than 11 m, as excessive proximity would not provide helpful validation information, and excessive distance increases the probability of photographing a completely different context. The visual vector calculation system was considered to be validated if the comparison between the magnitudes of the vector pairs met the following criteria: (i) r-squared > 0.80; (ii) r > 0.90; (iii) $p < 0.01$; and (iv) mean distance from the equality line < 0.05.

3.4. Representation of the Urban Green Vector Field

To test the hypothesis of a non-homogeneous distribution of greenery across different spatial directions, Moran's I and variogram analyses were applied, as explained in the following sections. The visual greenery vectors can be oriented differently in space, forming a vector field. To represent geographical points as points of a force field and, subsequently, correctly display the image of the vector field on a map, it was necessary to convert latitude and longitude coordinates into the Universal Transverse Mercator (UTM) projection system and normalize them in the range of values [0:1]. Once the urban green visual vectors were obtained for each observation point, the Python library Magpylib was used to generate the corresponding vector field, considering the application points as spherical magnets with a radius of 10^{-46} and a magnetization vector equal to the applied vector at the point. Matplotlib was used to represent the vectors' flow lines with a grid of 100×100 points and a density parameter of 50.

4. Case Study

This research focused on Milan Local Identity Nuclei 22 (NIL Città Studi) as a case study within the National Recovery and Resilience Plan (NRRP) framework. NILs, introduced in the Territorial Government Plan (PGT) in force since May 2020, can be defined as territorial units of Milan that include neighborhoods with specific and distinguishable characteristics, identified in terms of the concentrations of local commercial activities, green spaces, gathering places, and services, as well as elements of local identity [54]. The case study presented here is strongly characterized by the buildings of the Politecnico di Milano and the University of Milan, featuring green spaces such as Leonardo da Vinci Square, Piola Square, the Botanical Garden, Aspromonte Park Square, and Hawaii Gardens, and tree-lined avenues such as Bonardi Street, Bassini Street, Gaio Street, Pacini Street, and Romagna Street. This area is interesting because of the mixture of users, including university students, office workers, residents, and healthcare institutions, and the coexistence of roads for motorized transportation, trams, and bicycles.

5. Results

The number of points generated on the case study area street network was 938; 6 points were unavailable when querying the Street View API. The remaining 932 derived a set of 3728 pictures related to the four cardinal directions (Figure 3), subsequently processed using the ADE20K pre-trained model for image segmentation.

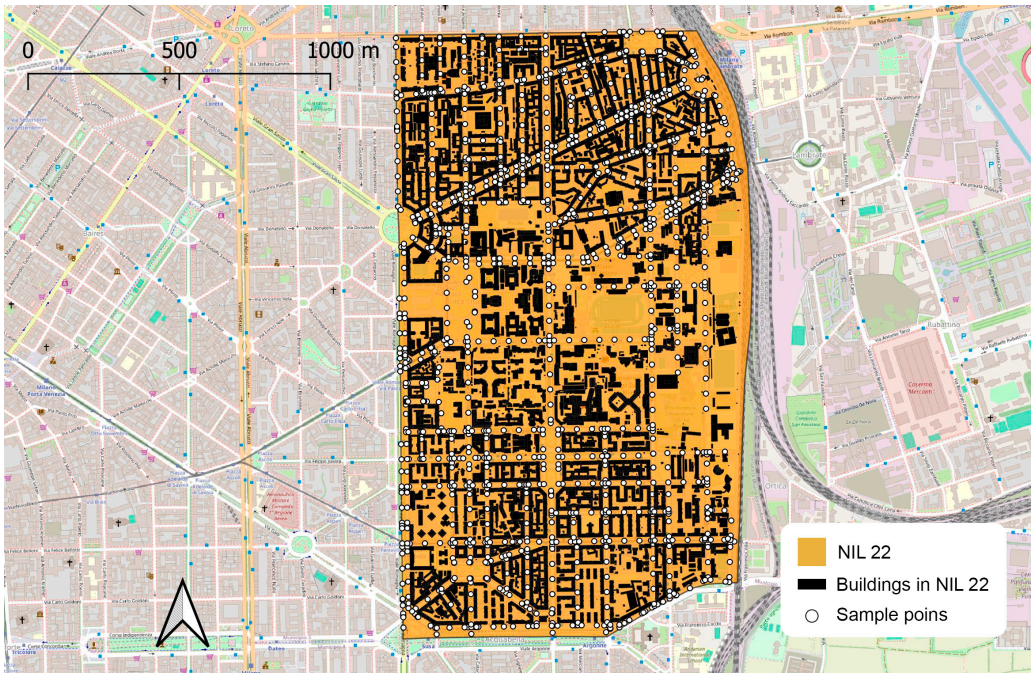

Figure 3. Orange shading is the area of NIL 22—Città Studi district. The white dots represent the location sent to Google Street™ to collect urban directional pictures. Source: Base map from Open Street Map™; elaboration by the author.

5.1. Validation of Image Segmentation and Segmentation Data Statistics for the Entire Neighborhood

Figure 4 illustrates the comparison between automatic and manual segmentation for data validation, highlighting the distinctions between the two methods. The figure includes a Street View image on the left, with the manually segmented areas overlaid in red (middle picture), and automatic segmentation on the right. This visual comparison provides a qualitative understanding of the differences in the segmentation results. Quantitatively, the analysis revealed a strong correlation between automatic and manual segmentation, with a correlation coefficient of 0.97 ($p < 0.001$), indicating a near-perfect linear relationship

between the two approaches. The R^2 value of 0.93 further supports the consistency between these methods, suggesting that the automatic process can explain 93% of the variability in manual segmentation. Furthermore, the mean deviation from the y = x line, representing perfect agreement, was calculated to be 0.019, indicating a minimal average error in the outputs of segmentation (Figure 5).

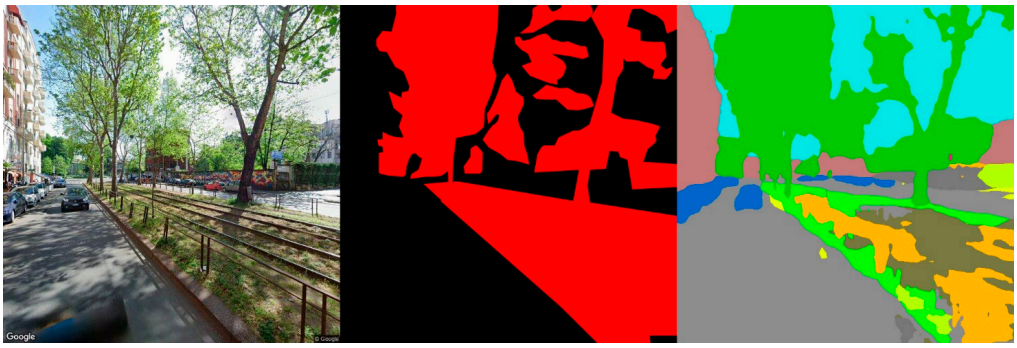

Figure 4. From left to right: original street view image, manual segmentation by the author to identify the areas of greenery (in red), and automatic image segmentation (greenery in green, street in grey, buildings in brown, sky in cyan, terrain in orange, sidewalk in dark gray, cars in blue). Source: Original image from Google Street View™; elaboration by the author.

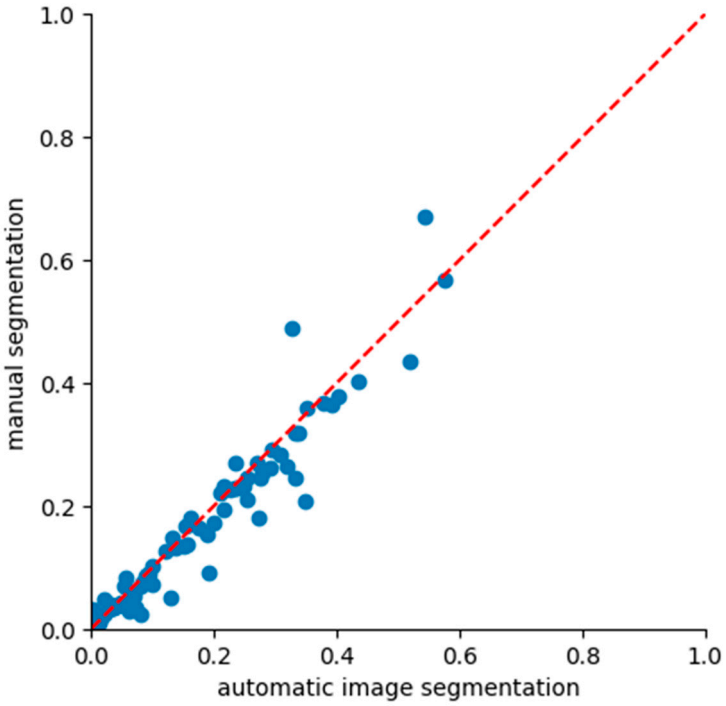

Figure 5. Distribution of percentages of greenery evaluated by automatic image segmentation and manual segmentation. The red dashed line shows the ideal data distribution in the case of a perfect match between the two methods.

5.2. Analysis of the Distribution of Greenery

The following equation shows that the decrease in visibility was slightly slower than the increase in greenery (Figure 6). This regression line was obtained by removing outliers from the dataset using the interquartile method and applying the Huber regressor [57] with limits of 10–90%:

$$\text{Buildings} = -0.92 * \text{Greenery} + 0.43.$$

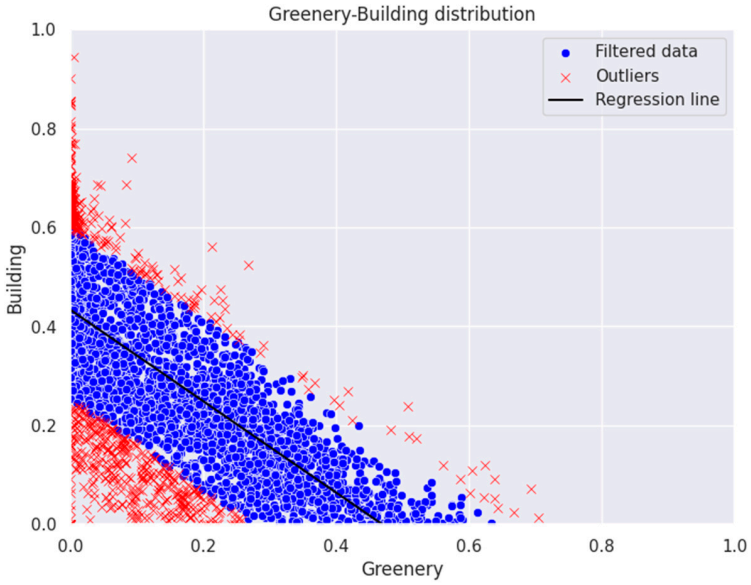

Figure 6. Average distribution of buildings versus the average distribution of greenery at each location. Red crosses are the points considered to be outliers after applying the interquartile method, blue dots are the points considered for linear regression, and the black line represents the regression trend line.

The percentage of vegetation, expressed as 360° GVI, goes from a minimum of 0.0% to a maximum of 47.3%, with a mean of 14.0% and a standard deviation of 10.8%.

When analyzing the GVI directional values of the area, some differences in the greenery ratio can be highlighted (Figure 7):

- GVI max: 0.473, mean: 0.140, std: 0.108;
- North max: 0.704, mean: 0.135, std: 0.147;
- East max: 0.634, mean: 0.142, std: 0.139;
- South max: 0.667, mean: 0.149, std: 0.149;
- West max: 0.588, mean: 0.134, std: 0.13.

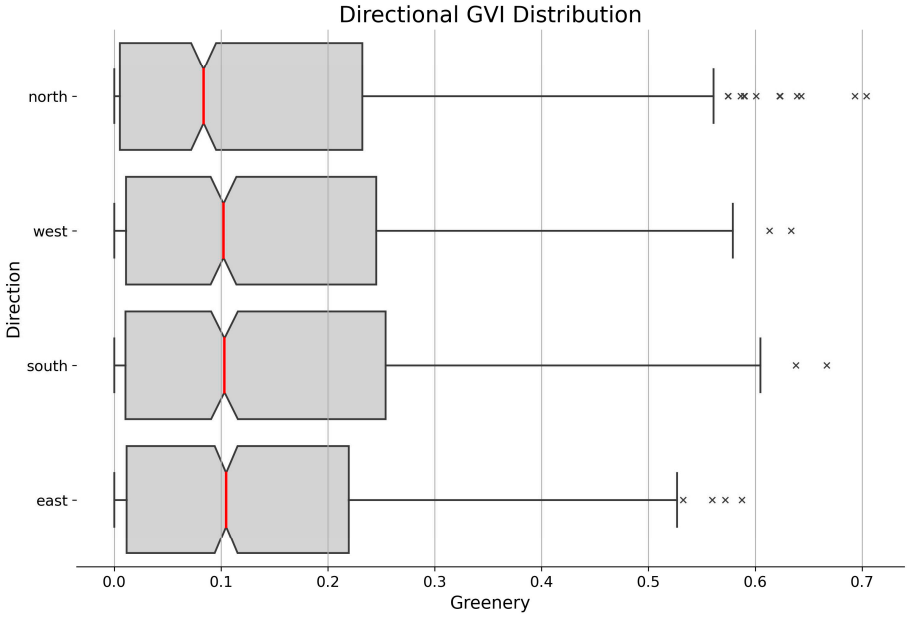

Figure 7. GVI index of the four cardinal directions. Most of the values range from 0 to 0.25 approximately; however, the values at the east are slightly more compressed compared with the other directions. The north's values reach the highest extension at 0.7.

This divergence of maximum values is also evident when comparing the distribution of GVI with the cardinal directions (Figure 8); the frequency of the 0.20 ratio is higher in GVI than in a single direction, and values greater than 0.40 are less represented. The overlap of the GVI and directional GVI data series makes it clear that in several locations, the highest greenery values are strongly oriented in a specific direction rather than equally distributed (Figure 9).

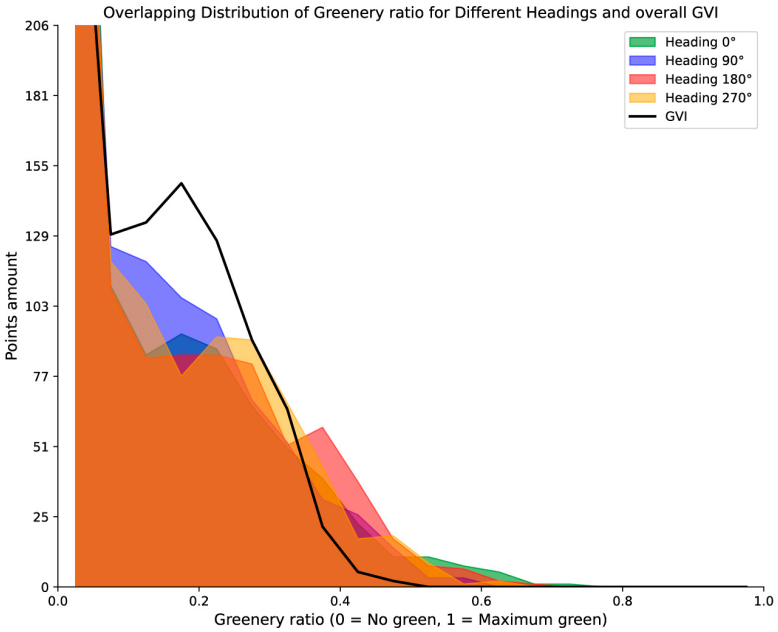

Figure 8. Overlapping of the directional distribution of greenery. The density chart represents how many points relate to a specific range of greenery ratios for each cardinal direction. Most cases present a low greenery ratio, followed by a long tail, showing a decrease in probability, while the amount of greenery increases. The black line represents the overall GVI value.

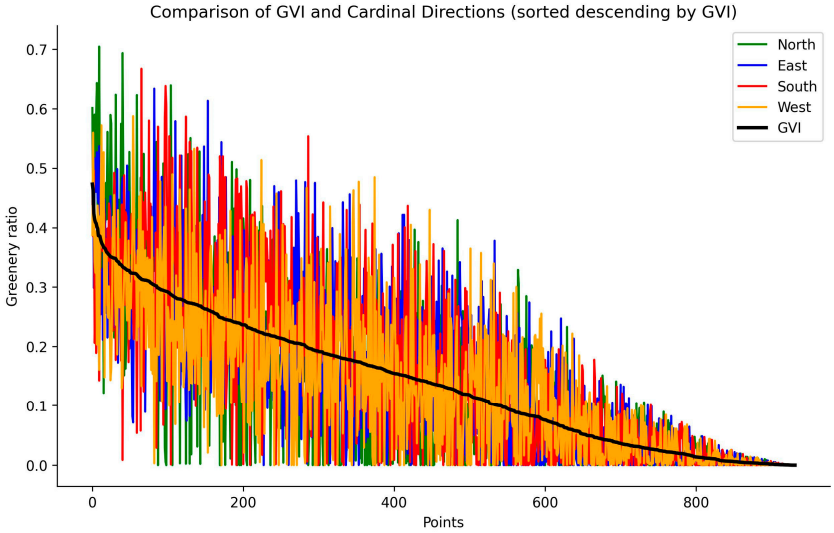

Figure 9. Line chart comparing the Green View Index (GVI) and the greenery ratio in four cardinal directions (north, east, south, and west), ordered by descending GVI. The chart shows that the directional values do not overlap at several points.

The Friedman test indicated significant differences in visible greenery among different cardinal directions (chi-square = 14.79, p-value = 0.0113), confirming that the spread of urban greenery varies among directional views. The difference in greenery is perceivable

between directional pairs, reaching up to 68 percentage points (Table 1). Dunn's post hoc test was used to identify which pairs of directions contributed most to this variability. The results of Dunn's test (Figure 10) show significant differences in greenery's visibility between specific pairs of cardinal directions, showing notable *p*-values below 0.05. In particular, north–east vs. south–west ($p = 0.003$) and north–south vs. south–west ($p < 0.001$), and north–south vs. south–east ($p = 0.031$). This pattern indicates that the visibility of greenery varies more prominently in some directions, with a significant asymmetry between northern and southern perspectives compared with other cardinal directions.

Table 1. Summary statistics of differences in greenery's visibility between pairs of cardinal directions, including absolute maximum differences, absolute mean values, and standard deviations.

Pair	Max Abs Diff.	Abs. Mean	Std. Dev.
North–south	0.6848	0.0146	0.1718
East–west	0.6306	0.0081	0.1595
North–east	0.3874	0.0077	0.1310
North–west	0.5438	0.0004	0.1493
South–east	0.5445	0.0069	0.1498
South–west	0.534	0.0150	0.1330

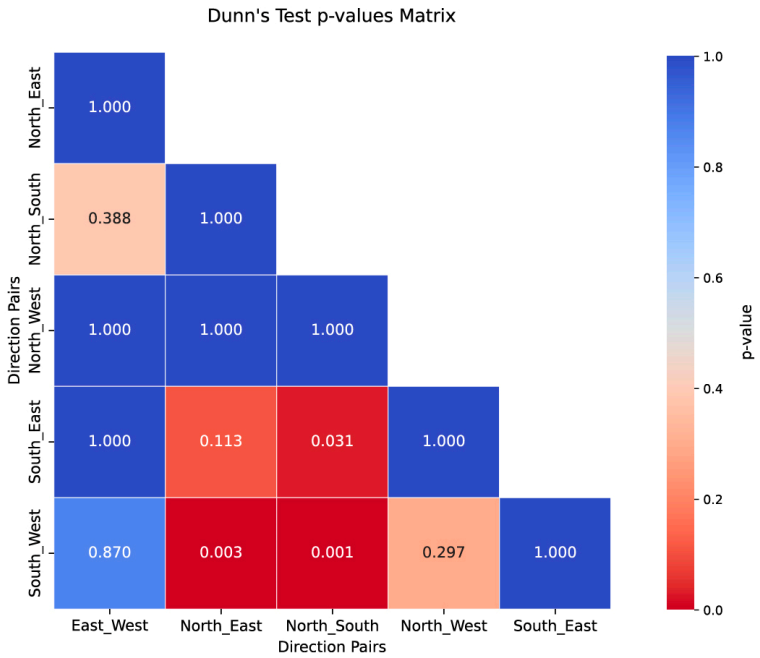

Figure 10. Heatmap showing *p*-values from Dunn's post hoc test comparing greenery's visibility differences between cardinal direction pairs. Red indicates significant differences ($p < 0.05$), and blue represents non-significant differences.

5.3. Anisotropy of Greenery and Representation of the Visual Greenery Field (VGF)

When conducting the Shapiro–Wilk test [58] on the greenery values, it was observed that the urban greenery in this area is not normally distributed (*p*-value < 0.05). An analysis of Moran's I [59] was performed on the directional subsets of the GVI values, applying the Queen method [60] for calculation of the weights. The results show a significant positive autocorrelation of greenery (*p*-value < 0.05). These data suggest the presence of concentrated peaks and long tails of uneven greenery values in the area examined (Table 2).

Table 2. The Shapiro-Wilk and Moran I results are shown in the rows with the related *p*-value. The four cardinal directions are organized by columns. The last column lists the average Shapiro-Wilk and Moran I values.

	Heading 0°	Heading 90°	Heading 180°	Heading 270°	Average
Shapiro–Wilk	0.85	0.89	0.88	0.89	0.88
p-value	<0.001	<0.001	<0.001	<0.001	<0.001
Moran's I	0.33	0.32	0.36	0.41	0.35
p-value	<0.001	<0.001	<0.001	<0.001	<0.001

As the variogram analysis shows (Figure 11), the greenery in this area follows an anisotropic organization, in which visual continuity spans from 404m at 22.5° north to 1076m at 67.5° north. This angle and length correspond to the main tree-lined avenues under examination.

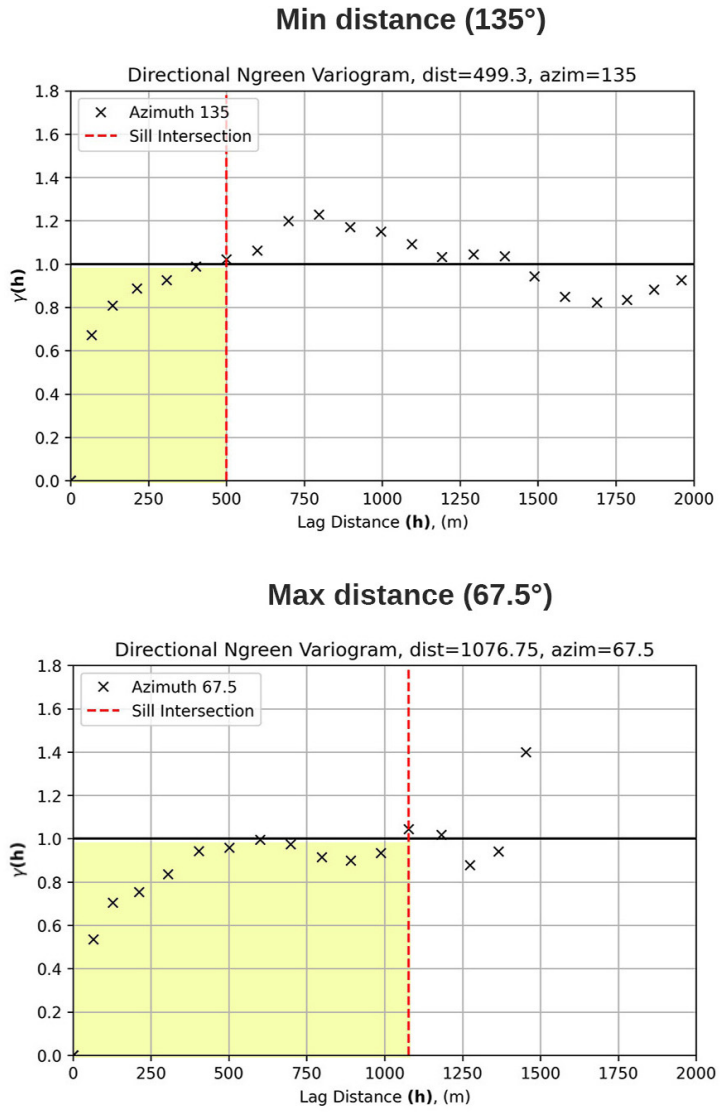

Figure 11. Variograms of the normalized values of the greenery ratio at different azimuth angles, specifically toward the maximum and minimum continuity distance. On the vertical axis, the semivariance value measures the degree of dissimilarity between pairs of data points separated by a certain distance (lag); the horizontal axis shows the lag distance, which is the separation distance

between pairs of data points. The black horizontal line represents a sill, that is, a limit beyond which data points are no longer spatially correlated, meaning that their dissimilarity no longer increases with distance; the red dashed vertical line represents the "range", the lag distance at which the variogram reaches the sill. Beyond this range, the data points in the acid green area are effectively uncorrelated.

The visual vectors, calculated as the vectorial sum of the cardinal greenery vectors, highlight relevant differences in the orientation and intensity, as shown in Figure 12. The mean orientation is 186.40 °N (std = 105.17 N), with a mean greenery ratio of 0.18 (std = 0.15). The vector calculation was validated by comparing the new sample points with the closest points in the original set. Following the validation procedure described earlier, the dataset of visual vectors of greenery was considered valid, as the resulting values fell within the established thresholds, meaning that the visual target to maximize the view of greenery is precisely located and stable even when shifting up to 10m from the original observation location:

- r: 0.92;
- r-squared: 0.83;
- *p*-value: 1.08×10^{-9};
- distance from y = x: 0.037.

Furthermore, the presence of vegetation in the four cardinal images changes in intensity when moving through the streets. Figure 13 shows how the visual vectors change direction and intensity across the district, while Figure 14 highlights where the GVI is more intense; comparing the two pictures, it is clear that the areal GVI does not provide the same information as the VGF.

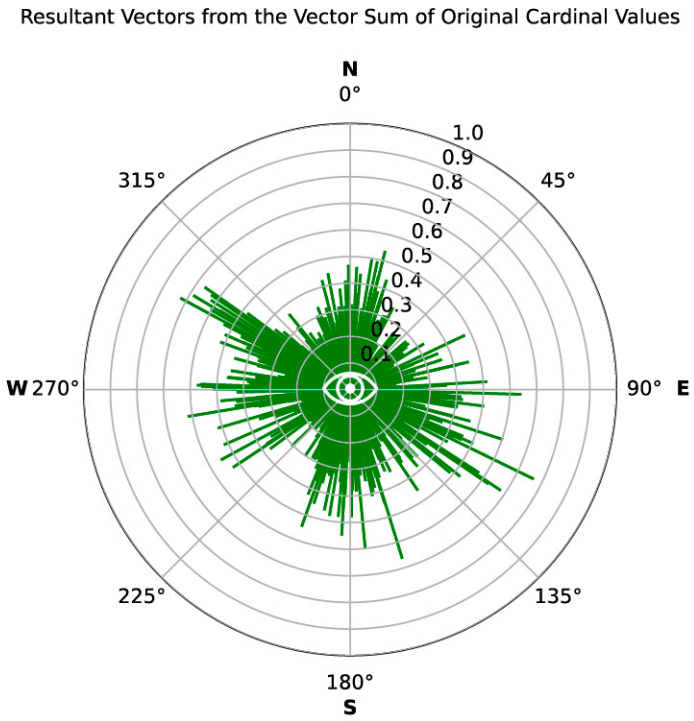

Figure 12. Polar chart of all visual greenery vectors for Città Studi. Each vector is calculated as the vectorial sum of the original cardinal values. The vector angles are oriented clockwise; the greenery ratio is represented by circles labeled 0 to 1, where 1 is the maximum possible intensity.

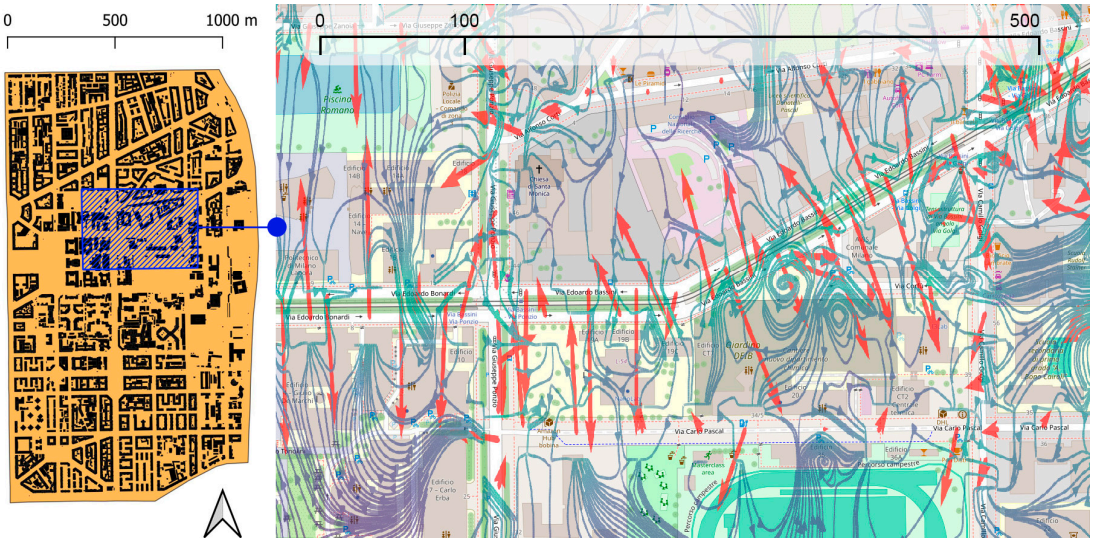

Figure 13. Visual greenery field. On the left is the key map of NIL 22, with the area shown on the right highlighted in blue. This area includes part of the Politecnico, the sports camp, and the main street. On the right, red arrows are the resulting view vectors; blue arrows are the streamlines of a potential green experiential connectivity field. Source: Base map from Open Street Map™; elaboration by the author.

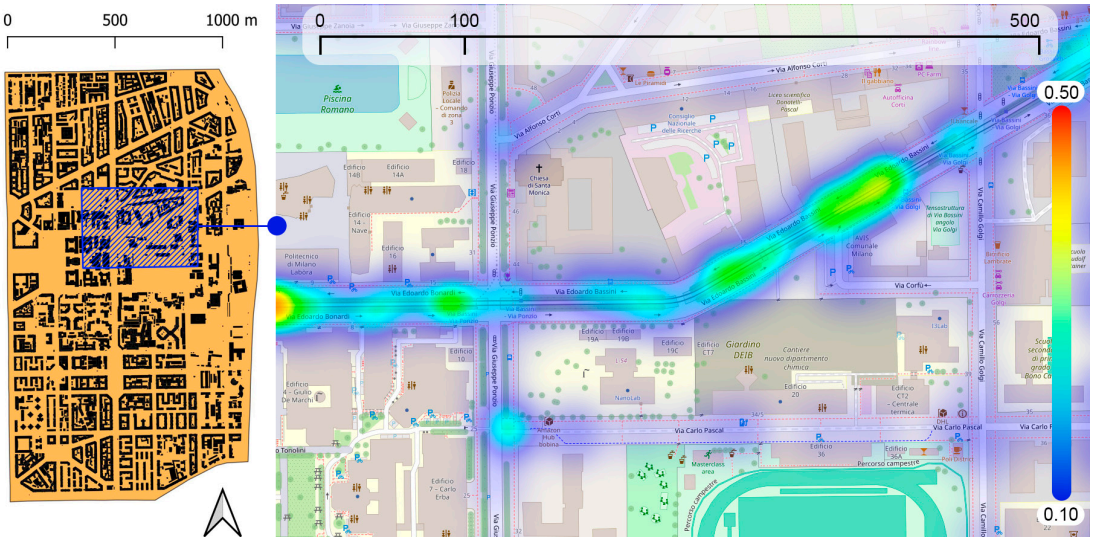

Figure 14. Representation of the GVI heatmap. On the left is the key map of NIL 22, with the area shown on the right highlighted in blue. This area includes part of the Politecnico, the sports camp, and the main street. On the right, this picture highlights that green elements tend to be concentrated along the main streets. Source: Base map from Open Street Map; elaboration by the author.

6. Discussion

The results of this study provide information on the visibility of urban greenery in different cardinal directions and its spatial distribution within the examined area. The first key finding is the unequal visibility of greenery, with significant variations between the north and south directions. These findings suggest that directional bias must be considered when assessing the visual perception of urban vegetation, as greenery is not evenly distributed in all orientations. Although urban vegetation is generally placed on the sides of the street, this is not always true, such as at a green roundabout or when a street reaches a park or a square. Previous studies focused on the one-directional view along a path or distributed 360° views, with panoramic approaches losing specific directional

information, while non-panoramic studies may fail to capture the broader context of urban greenery [31]. In particular, the vectorial analysis of green intensity across the four cardinal directions highlights the variation in green visibility depending on the viewer's orientation. This consideration suggests that using GVI as a unique value in the analysis can introduce bias in the evaluation of the urban green experience. This study overcomes these limitations by including all cardinal directions, synthesizing global information, and preserving directional data, thus capturing a comprehensive yet directionally detailed analysis of urban green. Geostatistical analyses, particularly Moran's I, revealed that greenery exhibits a spatial clustering tendency, with specific areas showing concentrated peaks. This positive autocorrelation is aligned with the observed heterogeneity in the visual distribution, which confirms that the greenery is not evenly spread. Furthermore, variograms in different azimuth directions reveal that the spatial continuity of greenery can vary significantly, ranging from 404 m to 1076 m depending on the direction, indicating a directional dependence on how greenery is distributed throughout the area.

The most intense vectors occur on tree-lined avenues along roads such as Edoardo Bassini Street, where the effect is amplified by the grass partially covering the tram tracks. This highlights an ambiguity: despite the abundance of greenery, the usability of these green spaces is limited by physical barriers such as tram tracks and roads, which detract from their immersive quality. An exception is Pacini Street, near the Piola metro station, where the section is such that it can offer facilities for sociality. This observation goes beyond the scope of several studies [26,33,34,36,38–42], which measured GVI in different cities but did not address the anisotropic distribution of greenery or its potential barriers to usability. The angular drift from the street axis does not occur facing green roundabouts such as Piola Square, where the presence of greenery is directly observable from radial roads. Analysis of the directional differences in the visibility of greenery further supports the notion of an uneven visual field of greenery. The results of the Friedman test and subsequent post hoc analysis show that specific direction pairs, particularly those involving south-facing views, exhibit the most significant variability. This suggests that individuals' experience of urban greenery is highly dependent on their orientation within the city. The representation of visible green as a vector field shows areas where the opposition of close visual directions generates a sort of turbulence. In contrast, aligned field bands show areas where the vectors' directions are coherent between opposing zones. Changes in the vectors' alignment can suggest incongruency between parts of the neighborhood that are not always mutually connected by crossings and that do not allow for a continuous green immersion experience; a particular case where visual connection corresponds to a possibility of movement through the greenery is constituted by the area of the Politecnico di Milano's rectorate, where it is possible to pass from one perimeter tree-lined avenue to another by walking through the internal campus gardens.

It is worth noting that the sum of vectors following image segmentation implies the existence of two possibilities of zero values: (a) a system at rest, with a lack of green in all directions; (b) a balanced system, with the identical presence of green in all directions. The second possibility is unlikely because the pictures represent an urban environment seen from a street; however, these boundary conditions are considered acceptable, as the research aimed to identify the preferential orientation toward specific directions; thus, obtaining the zeroed vector in the possible presence of 360° of green represents indifference toward any specific direction. Moreover, the vectorial representation is to be considered complementary to the areal one. However, it is important to acknowledge that this vectorial approach, while informative, does not fully capture the complexity of how humans perceive or access greenery in real-world environments. Human perception is influenced by multiple sensory and contextual factors that go beyond the directional quantification of green visibility, and this limitation should be recognized. It is also important to emphasize that this type of analysis is not intended to replace the GVI but to complement it by providing additional information on directional preferences. Relying on an omnidirectional GVI, especially over large areas, risks losing important details about the local distribution of greenery.

A 360° average GVI may not accurately reflect the urban layout at specific observation points. For example, different scenarios, such as a single tree in a built environment versus multiple small plants on facades, can produce similar GVI values despite differing visually. Although the areal GVI derives from directional information, the differences in the directional distribution of greenery are crucial to understanding the perceptual reality of urban spaces, indicating that GVI alone may not capture all the relevant information.

Therefore, the vectorial representation of urban green visual elements provides information on (i) the prevailing visual direction at a point that maximizes the view of green, (ii) the intensity of green in that direction compared with the surrounding elements, and (iii) the directional coherence between neighboring places. In response to the first research question, the proposed vector-based method quantified the intensity and spatial distribution. This approach allows for a clearer understanding of directional visibility, showing significant differences among the cardinal directions. This directional specificity is essential to represent urban green spaces with more precision, which the traditional GVI, as an omnidirectional measure, fails to capture. Regarding the second research question, vector representation provided information on the directional coherence across the area, highlighting zones of alignment and turbulence across the urban landscape. The alignment of vectors' directions between adjacent areas reflects the congruence of green visibility, which is not easily observable by omnidirectional GVI alone. This allows for a more nuanced interpretation of how greenery is experienced in different parts of the urban fabric.

This type of analysis is tied to panoramic photography conducted along the road axis and, therefore, does not allow for an exact evaluation of perception from different positions, such as that of a pedestrian on the sidewalk. The images were all captured during daylight hours, so assessing how perception varies under special lighting conditions such as dawn or dusk is impossible. Additionally, it was not possible to set different dates to retrieve shots in different seasons. The height of the viewpoint is higher than the average height of a standing person or a driver on the wheel, since it was taken from above the roof of a car; this may distort the human viewpoint. The fineness of viewpoints' discretization along the path can vary the representation, providing more detailed information and, therefore, more localized phenomena. Future work on urban perception would benefit from considering the effects of continuous exposure to greenery compared with punctuated or fragmented ones by adopting such a method to select paths with different qualities and features. Furthermore, future research could focus on integrating different models to quantify urban greenery by combining satellite images with street-level greenery information, such as the GVI and NDVI. This approach should also incorporate the directional aspects highlighted in this study to create a three-dimensional view of the urban environment. Furthermore, recent developments in deep learning processes present an opportunity to handle large-scale geospatial datasets, enabling more refined predictions and analyses, mainly when dealing with detailed urban data.

Funding: This work has been developed within the MUSA—Multilayered Urban Sustainability Action—project, funded by the European Union NextGenerationEU, under the National Recovery and Resilience Plan (NRRP) Mission 4 Component 2 Investment Line 1.5: Strengthening of research structures and creation of R&D "innovation ecosystems", set up of "territorial leaders in R&D".

Institutional Review Board Statement: Not applicable.

Informed Consent Statement: Not applicable.

Data Availability Statement: Data are available on request and belong to wider, funded ongoing research.

Conflicts of Interest: The author declares no conflicts of interest.

Appendix A. Scoping Review

The following appendix details the structured approach used for the literature review. First, the query structures employed for the Scopus, Web of Science, and Dimensions

databases are presented. The PRISMA method was used to identify relevant publications. Finally, the identified dataset was validated based on the principle of saturation, ensuring comprehensive coverage of the topic. The search queries were designed to identify peer-reviewed publications related to the Green View Index (GVI) from 2013 to 2023. The Scopus query is focused on the "green view index" and was limited to journal articles and reviews published in English. The Web of Science search followed a similar structure, refining the results by relevance. For dimensions, the term "streetview" was added to narrow the broad scope of the initial results. The SPIDER framework inspired the conceptual query framework [61,62]: S, sample; PI, phenomenon of interest; D, study design; E, evaluation; R, research type. The "publication type" replaced the "research type" section, and the evaluation was subsequently carried out following the PRISMA protocol; the queries were not limited in terms of the design of the study (Figure A1).

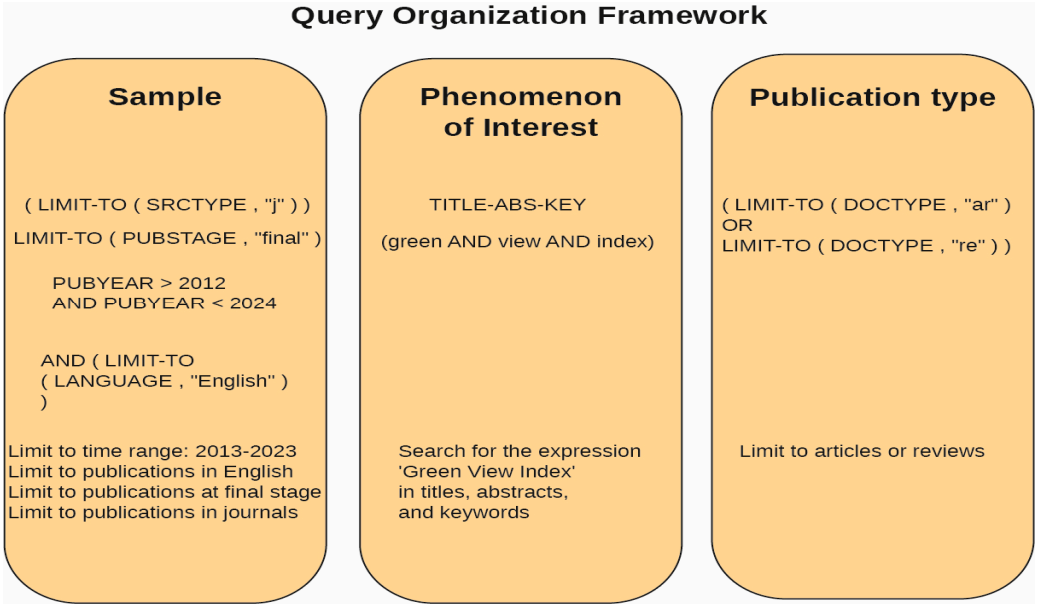

Figure A1. Query organization framework. The three blocks are related to the literature sample, the phenomenon of interest, and the type of publications to be included in the search.

Scopus query: TITLE-ABS-KEY (green AND view AND index) AND PUBYEAR > 2012 AND PUBYEAR < 2024 AND (LIMIT-TO (SRCTYPE, "j")) AND (LIMIT-TO (LANGUAGE, "English")) AND (LIMIT-TO (PUBSTAGE, "final")) AND (LIMIT-TO (DOCTYPE, "ar") OR LIMIT-TO (DOCTYPE, "re")).

Web of Science (WOS) query: https://www.webofscience.com/wos/woscc/summary/9e9f03ab-6caa-4646-8a7e-99b127ef7add-af2a77e2/relevance/1 (accessed on 28 October 2023).

Dimensions query: "green view index streetview" in full data; publication year was 2023 or 2022 or 2021 or 2020 or 2019 or 2018 or 2017 or 2016 or 2015 or 2014 or 2013; publication type was article or chapter.

Due to the extensive nature of the results for dimensions, it was necessary to introduce the keyword 'streetview' to obtain a more focused outcome compared with the search queries.

The results of these three databases were merged into a single dataset from which duplicates were removed (Table A1). The saturation principle was followed to validate the dataset, adopting Google Scholar™ as a comparison set. Details of the procedure are provided on the following pages, and the schema is shown in Figure A2. The three publications' dataframes obtained were concatenated, obtaining 1810 items; 47 items have been removed due to missing DOI information; out of the remaining 1763, 447 duplicates were removed. After this filtering, the resulting dataframe contained 1316 items. The process of including datasets to obtain a comprehensive framework could virtually continue without limit; for

this reason, it was necessary to establish a threshold of validity for the items collected. The validation of the items was achieved using the saturation principle applied through a comparison of Google Scholar™ (GS) with the final dataset of publications derived from the previous phases. The saturation check used a dataset not initially included to verify the percentage of duplicates that would appear in the original set by merging a new set of items. The comparison was processed under two different conditions: (i) the complete GS dataframe; (ii) the GS dataframe filtered by citations per year (CpY), considering the same threshold that was applied to the original dataframe (CpY = 10). The percentage must be >75% for the complete dataframe and >60% for the filtered dataframe to be valid. The following are the levels overlapping for comparing the DOI in the two datasets:

- Overlapping percentage of whole GS = 83.33% (saturation confirmed);
- Overlapping percentage of filtered GS = 66.66% (saturation confirmed).

This means that including other sources would produce a nearly identical item list to the one initially chosen to represent the state-of-the-art in this field.

Google Scholar™ Query: The search on Google Scholar™ was conducted using Harzing's Publish or Perish tool v. 8.9.4538.8589 2023.07.07.1629 [63] by setting the following parameters:

- Title: green view index;
- Keywords: green view index;
- Years: from 2013 to 2023;
- Maximum results: 200;
- No patents.

Citations per year filtering was used to obtain the most influential publications, and a threshold of 10 citations per year was applied to be included in the screening phase. The resulting subset contained 159 items (1157 were removed).

Title screening: In this phase, the relevant terms were street view, street greenery, Green View Index, view factors, street-level images, and eye-level greenness. Other excluded publications were on satellite images, remote sensing, and crop health assessment. Title screening resulted in 35 items (124 were removed).

Abstract screening: In this phase, publications on transport not explicitly citing the GVI and publications not implying street-eye level images were excluded. Abstract screening resulted in 32 items (3 were removed).

Full text screening: In this phase, a publication was excluded because it was not related to the research questions.

To better describe the framework of the current research, one publication that was not initially included in the original dataframe was added; Table A2 reports on these publications with their motivations. The ultimate set of publications included 32 items.

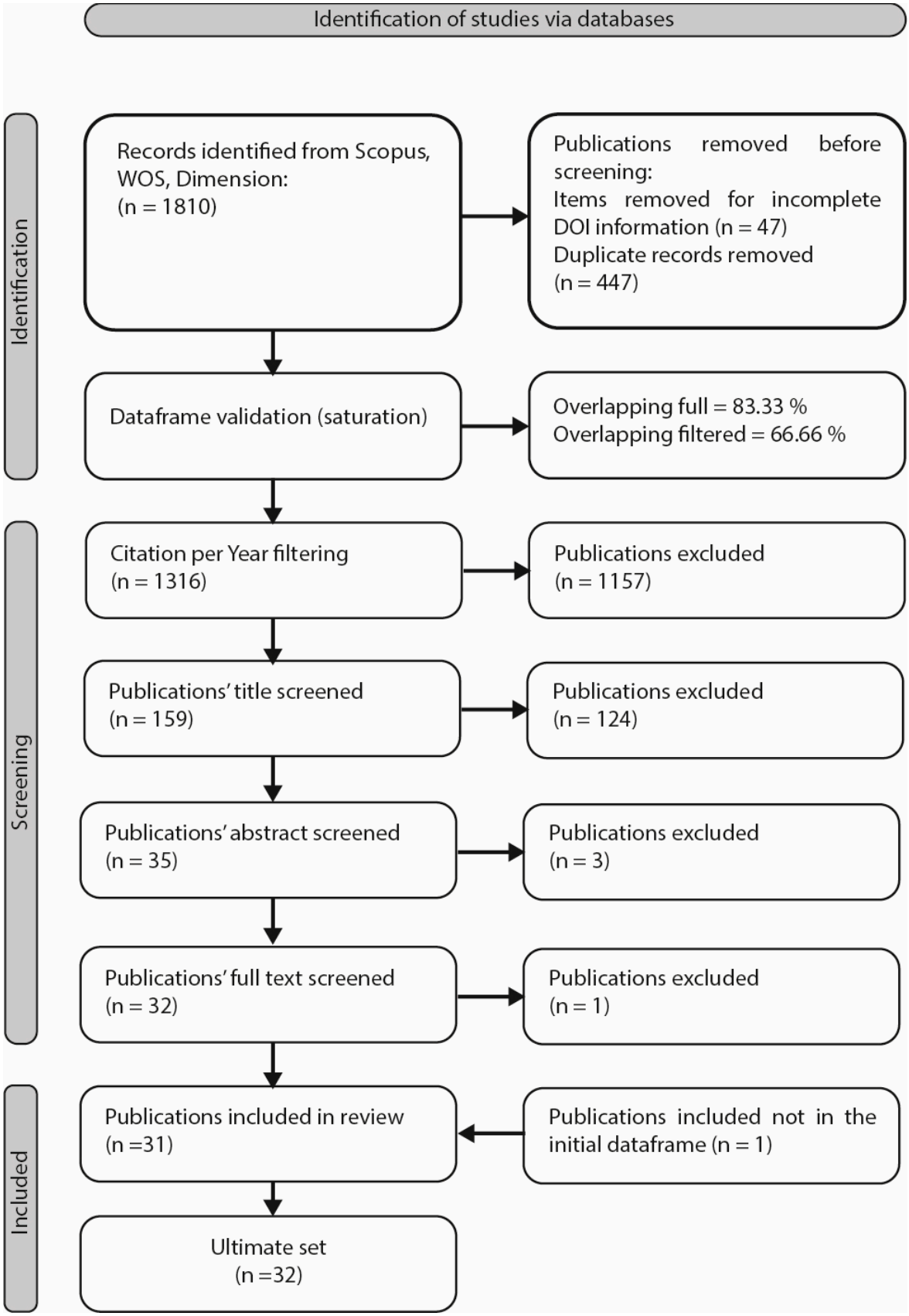

Figure A2. Literature review diagram for the Green View Index. This schema is based on the Preferred Reporting Items for Systematic Reviews and Meta-Analyses (PRISMA) flow chart [26]. Retrieved on 2 November 2023, from http://prisma-statement.org.

Table A1. List of publications included after full test evaluation.

Title	Authors	Year	Description
Assessing street-level urban greenery using Google Street View and a modified green view index [26]	Li, Xiaojiang; Zhang, Chuanrong; Li, Weidong; Ricard, Robert; Meng, Qingyan; Zhang, Weixing	2015	Automated calculation of the GVI and its rationalization compared with the previous work in 2009
View-based greenery: A three-dimensional assessment of city buildings' green visibility using Floor Green View Index [33]	Yu, SY; Yu, BL; Song, W; Wu, B; Zhou, JH; Huang, Y; Wu, JP; Zhao, F; Mao, WQ	2016	Three-dimensional evaluation of greenery
How green are the streets? An analysis for central areas of Chinese cities using Tencent Street View [34]	Long, Ying; Liu, Liu	2017	Using conventional methods is generally time-consuming and expensive. To address this issue, the authors developed an automatic method using a street-view service while also borrowing and modifying ideas from existing studies
Green streets—Quantifying and mapping urban trees with street-level images and computer vision [38]	Seiferling, Ian; Naik, Nikhil; Ratti, Carlo; Proulx, Raphäel	2017	Quantifying the amount and distribution of trees in cities
Quantifying street tree regulating ecosystem services using Google Street View [39]	Richards, Daniel R.; Edwards, Peter J.	2017	The study analyses hemispherical photographs extracted from Google Street View to quantify the proportion of green canopy coverage at 50 m intervals across more than 80% of Singapore's road network and estimates the proportion of annual radiation that would be blocked from reaching ground level by the canopy. The study aimed to map the provision of street trees' ecosystem services and prioritize areas for new planting by identifying streets or street sections with low shading
How green are the streets within the sixth ring road of Beijing? An analysis based on Tencent Street View pictures and the Green View Index [35]	Dong, RC; Zhang, YL; Zhao, JZ	2018	This article aimed to quantify the street greenery in the sixth ring road in Beijing, analyze the relations between road parameters and the GVI, and compare the visible greenery of different types of roads
Impacts of street-visible greenery on housing prices: Evidence from a hedonic price model and a massive street view image dataset in Beijing [40]	Zhang, YL; Dong, RC	2018	The authors selected 25 variables that were classified into three categories (location, housing, and neighborhood characteristics) and introduced an index called the horizontal green view index (HGVI) into a hedonic pricing model to measure the value of visual perceptions of street greenery in neighboring residential developments
Mapping sky, tree, and building view factors of street canyons in a high-density urban environment [36]	Gong, Fang-Ying; Zeng, Zhao-Cheng; Zhang, Fan; Li, Xiaojiang; Ng, Edward; Norford, Leslie K.	2018	This study aimed to develop an approach to estimate and map the SVF, TVF, and BVF of street canyons in complex urban living environments, such as high-density urban areas in Hong Kong
The effect of street-level greenery on walking behavior: Evidence from Hong Kong [44]	Lu, Yi; Sarkar, Chinmoy; Xiao, Yang	2018	This study highlighted the impact of eye-level street greenery on the decision to walk and the total walking time for a large urban population of Hong Kong
Using deep learning to examine street view green and blue spaces and their associations with geriatric depression in Beijing, China [28]	Helbich, M; Yao, Y; Liu, Y; Zhang, JB; Liu, PH; Wang, RY	2019	This study was among the first to examine the link between mental disorders (that is, depressive symptoms) and exposure to natural environments at the street level among elderly people in China

Table A1. *Cont.*

Title	Authors	Year	Description
Associations between overhead-view and eye-level urban greenness and cycling behaviors [43]	Lu, Y; Yang, YY; Sun, GB; Gou, ZH	2019	The article's main objective was to examine the association between urban greenness and the odds of cycling for Hong Kong participants, using two ways of measuring urban greenness: overhead-view greenness and eye-level street greenness. The article also aimed to investigate the impacts of the activity-influencing built environment and individual-level covariates on cycling behavior. The findings of the study could help planners and designers build a cycling-friendly city by improving citizens' daily exposure to urban greenness
Using Google Street View to investigate the association between street greenery and physical activity [45]	Lu, Yi	2019	This discusses the association between street greenery and physical activity in a study conducted in Hong Kong. The study used free Google Street View images to assess the quantity and quality of street greenery, and associated them with the recreational physical activity in green outdoor environments of 1390 participants in 24 housing estates in Hong Kong. Multilevel regression models revealed that the quality and quantity of street greenery were positively linked to recreational physical activity
Evaluating street view exposure measures of visible green space for health research [27]	Larkin, A; Hystad, P	2019	This examined how exposure to green space or natural environments can affect physical and mental health outcomes. The study concluded that urban green spaces are associated with multiple physical and mental health benefits, but they are often difficult to measure accurately. The authors used Google Street View (GSV) technology to collect images from Portland, Oregon, and map out the amount of green space in each image, calling it the Green View Index (GVI). They also compared their GVI findings with traditional measures of green space exposure such as the satellite-based normalized difference vegetation index (NDVI), % tree cover, % green space, % street tree buffering, distance to parks, and several neighborhood socioeconomic variables
Perceptions of built environment and health outcomes for older Chinese in Beijing: A big data approach with street view images and deep learning technique [8]	Wang, Ruoyu; Liu, Ye; Lu, Yi; Zhang, Jinbao; Liu, Penghua; Yao, Yao; Grekousis, George	2019	The article discussed the association between the attributes of the built environment and health outcomes for older adults, focusing on perceptions of the built environment. The study used street view images and deep learning techniques to assess perceptions of the built environment for a large-scale study area. The results suggest that perceptions of safety, depression, beauty, wealth, boredom, and liveliness are all associated with the physical and/or mental health outcomes of older adults

Table A1. *Cont.*

Title	Authors	Year	Description
Measuring daily accessed street greenery: A human-scale approach for informing better urban planning practices [5]	Ye, Yu; Richards, Daniel; Lu, Yi; Song, Xiaoping; Zhuang, Yu; Zeng, Wei; Zhong, Teng	2019	This was a research article on a measurement approach for quantifying urban residents' daily exposure to eye-level street greenery by integrating high-resolution measurements of both greenery and accessibility. The proposed approach used Google Street View (GSV) images and street networks collected from Open Street Map (OSM) and combined them with machine learning algorithms to accurately measure visible greenery. The integration of greenery and accessibility helps to measure greenery from a human-centered perspective, and it provides a tool for urban planners to prioritize planning interventions
A review of urban physical environment sensing using street view images in public health studies [49]	Kang, Yuhao; Zhang, Fan; Gao, Song; Lin, Hui; Liu, Yu	2020	This article reviewed urban physical environment sensing using street view images in public health studies. The article systematically reviewed the use of street view images to detect urban environments in public health studies, describing the characteristics of street view images and summarizing the challenges of quantifying urban environments in terms of data and methodology. The manuscript included a discussion of future research directions that would benefit public health research and practices in urban environment research
Examining the spatial distribution and temporal change of the green view index in New York City using Google Street View images and deep learning [41]	Li, XJ	2021	This study mapped the spatial distribution of and temporal changes in street tree canopies using ground-based images in New York City
The distribution of greenspace quantity and quality and their association with neighbourhood socioeconomic conditions in Guangzhou, China: A new approach using deep learning method and street view images [42]	Wang, RY; Feng, ZQ; Pearce, J; Yao, Y; Li, XJ; Liu, Y	2021	This study developed a new machine learning method to assess the quality of green space based on street view images collected from Guangzhou, China. It also examined whether disparities in greenspace exposure are linked to the neighborhood's socioeconomic status (SES)
Street view images in urban analytics and GIS: A review [31]	Biljecki, Filip; Ito, Koichi	2021	This provided a comprehensive systematic review of the state of the art of how street-level images are currently used in studies about the built environment. The article outlined how street-level images are now an entrenched component of urban analytics and GIScience; most of the research relies on data from Google Street View, which are used across many domains with numerous applications
Using Google Street View images to capture micro built environment characteristics in drug places, compared with street robbery [7]	Zhou, Hanlin; Liu, Lin; Lan, Minxuan; Zhu, Weili; Song, Guangwen; Jing, Fengrui; Zhong, Yanran; Su, Zihan; Gu, Xin	2021	The authors calculated safety scores, extracted physical elements, and built logistic regression models to examine the impact of the micro-built environment's variables on drug activities. The results suggested that less place management and higher accessibility increase the risk of drug activities. The study also suggested that these street-view variables may generally apply to other types of crime research in the micro-built environment

Table A1. *Cont.*

Title	Authors	Year	Description
Can't see the wood for the trees? An assessment of street view- and satellite-derived greenness measures in relation to mental health [51]	Helbich, Marco; Poppe, Ronald; Oberski, Daniel; van Emmichoven, Maarten Zeylmans; Schram, Raoul	2021	The article examined the association between urban greenness and mental health using different greenness metrics, including remotely sensed and street view measurements. The results indicated that different methods of measuring greenness may capture different aspects of greenery in urban environments. However, these differences in the exposure metrics did not translate into significant associations with mental health outcomes
Modelling and mapping eye-level greenness visibility exposure using multisource data at high spatial resolutions [32]	Labib, SM; Huck, JJ; Lindley, S	2021	This article introduced a methodology for modeling and mapping eye-level greenness visibility and exposure at high spatial resolutions. The methodology used multisource spatial data and applied viewshed analysis with a distance decay model. The aim was to capture eye-level greenness visibility and exposure at observers' locations on the ground. The article compared top-down greenness exposure metrics with eye-level greenness exposure metrics
Assessing bikeability with street view images and computer vision [29]	Ito, Koichi; Biljecki, Filip	2021	This discussed the use of street view images (SVI) and computer vision (CV) to evaluate bikeability, which was defined as the extent to which cycling is facilitated in urban areas. An exhaustive index of bikeability composed of 34 indicators was developed and applied in Singapore and Tokyo to evaluate the usefulness of these technologies. The results suggested that SVI and CV are adequate for evaluating bikeability, present a contribution to transportation and analytics, and are scalable enough to widely assess the appeal of cycling
Analyzing the effects of Green View Index of neighborhood streets on walking time using Google Street View and deep learning [47]	Ki, D; Lee, S	2021	This discussed the effects of greenery on walking time and the importance of examining the relationship between urban greenery and walking behavior from multiple angles. It utilized Google Street View (GSV) and deep learning to calculate the Green View Index (GVI) by semantic segmentation, referring to greenness from the visual perspective of pedestrians. The GVI was found to be more closely associated with walking time than traditional greenery variables from an overhead perspective, such as park areas and the normalized difference vegetation index (NDVI)
Relative importance of quantitative and qualitative aspects of urban green spaces in promoting health [50]	Zhang, LQ; Tan, PY; Richards, D	2021	This research examined the relative importance of quantitative and qualitative aspects of urban green spaces (UGS) in the promotion of health. The study examined relationships between multiple UGS provision indicators and mental and general health outcomes in Singapore
Urban neighbourhood environment assessment based on street view image processing: A review of research trends [52]	He, Nan; Li, Guanghao	2021	The selected articles were classified into 5 broad categories and 15 subcategories of research directions, with research methods including reviews, experimental-based research, simulations, experiments + simulations, and surveys/audits. The review elaborated on the themes and content trends in the use of street views in the study of urban neighborhood environments

Table A1. *Cont.*

Title	Authors	Year	Description
Quantifying the shape of urban street trees and evaluating its influence on their aesthetic functions based on mobile lidar data [37]	Hu, T.; Wei, D.; Su, Y.; Wang, X.; Zhang, J.; Sun, X.; Liu, Y.; Guo, Q.	2022	The proposed method for assessing the esthetic functions of street trees quantified the shape of greenness, inspired by the skyline's esthetics. The authors used LIDAR data and panoramic images to extract the canopy line, identifying peaks and gaps, and six indexes to describe the fluctuations and continuities of street canopy lines. They analyzed the abundance and spatial distribution of these indexes alongside esthetic survey responses, finding significant correlations with human perception. Compared with indexes of the amount of greenness, these shape indexes have a stronger influence on the esthetic beauty of street trees, differing from previous studies focused solely on ecological services
Investigating pedestrian-level greenery in urban forms in a high-density city for urban planning [22]	Hua, J.; Cai, M.; Shi, Y.; Ren, C.; Xie, J.; Chung, L.C.H.; Lu, Y.; Chen, L.; Yu, Z.; Webster, C.	2022	The authors developed the Green View Factor (GVF) to measure pedestrian-level street greenery in Hong Kong using Google Street View (GSV) images. The study revealed significant variability in greenery across different urban forms, with older, high-density areas showing less greenery, often correlating with lower incomes. The GVF was strongly correlated with satellite-derived vegetation metrics (NDVI), though this varied by urban form. The findings suggested that the combination of multiple methods of assessing greenery is essential for a comprehensive understanding of the distribution of greenery in urban settings and can guide equitable urban planning strategies for high-density cities
Exploring the associations between neighborhood greenness and level of physical activity of older adults in Shanghai [46]	Xiao, Y.; Miao, S.; Zhang, Y.; Xie, B.; Wu, W.	2022	Green space was shown to be effective in encouraging people to undertake physical activity, while for older people, health conditions and socioeconomic characteristics were stronger influences on the amount of physical activity performed
Analyzing the effects of nature exposure on perceived satisfaction with running routes: An activity path-based measure approach	Huang, D.; Jiang, B.; Yuan, L.	2022	This discussed the positive association between running satisfaction and nature exposure, including eye-level greenness, top-down greenness, and blue space density. The study utilized an activity path-based measure approach using Public Participation GIS (PPGIS) to investigate these associations
Do emotional perceptions of visible greeneries rely on the largeness of green space? A verification in Nanchang, China [48]	Huang, S.; Zhu, J.; Zhai, K.; Wang, Y.; Wei, H.; Xu, Z.; Gu, X.	2022	This discussed a study that investigated the effect of the size of green spaces on the emotional perceptions of visitors in Nanchang City, China. The study used machine learning and sentiment analysis to analyze panoramic photos and visitors' facial expressions in green spaces. The results suggested that increasing the Panoramic Green View Index (PGVI) in green spaces can lead to more positive emotions in visitors

Table A2. Publications included in the final set of literature.

Reference	Motivation
Yang, J., Zhao, L., Mcbride, J., & Gong, P. (2009). Can you see green? Assessing the visibility of urban forests in cities. Landscape and Urban Planning, 91(2), 97–104. https://doi.org/10.1016/j.landurbplan.2008.12.004 [24]	This article is the origin of the GVI research.

Appendix B. Materials and Tools

The analyses were conducted using various systems, including drafting custom codes and scripts developed by the author. All GIS processing was performed using shapefiles provided by the geoportal of the Milan Municipality, employing QGIS 3.30.3-'s Hertogenbosch software. Image processing was performed using Python in the Google Colab™ environment; specifically, the Google Streetview 1.2.9 and GluonCV 0.10.5 libraries were used. For the validation of the results of segmentation, the opencv-python 4.8.1.78 library was adopted. The semantic dataset used for the image segmentation model was the ADE20K dataset [56] developed by MIT. The Magpylib 4.4.0 library [64] and the Matplotlib 3.8.1 streamplot function were used to represent the vector field. Mapping representation was accomplished using the folium 0.14 library with Open Street Map base layers. Regarding statistical calculations, the Moran's I calculation was performed using the esda 2.5.1 library, and the Shapiro–Wilk tests were conducted using the Scipy 1.11.3 library.

References

1. United Nations, N.Y., NY, USA, Cities—United Nations Sustainable Development Action 2015. Available online: https://www.un.org/sustainabledevelopment/cities/ (accessed on 1 October 2024).
2. Bambó Naya, R.; de la Cal Nicolás, P.; Díez Medina, C.; Ezquerra, I.; García-Pérez, S.; Monclús, J. Quality of Public Space and Sustainable Development Goals: Analysis of Nine Urban Projects in Spanish Cities. *Front. Archit. Res.* **2023**, *12*, 477–495. [CrossRef]
3. Wang, W.; Lin, Z.; Zhang, L.; Yu, T.; Ciren, P.; Zhu, Y. Building Visual Green Index: A Measure of Visual Green Spaces for Urban Building. *Urban For. Urban Green.* **2019**, *40*, 335–343. [CrossRef]
4. Bolte, A.-M.; Niedermann, B.; Kistemann, T.; Haunert, J.-H.; Dehbi, Y.; Kötter, T. The Green Window View Index: Automated Multi-Source Visibility Analysis for a Multi-Scale Assessment of Green Window Views. *Landsc. Ecol.* **2024**, *39*, 71. [CrossRef]
5. Ye, Y.; Richards, D.; Lu, Y.; Song, X.; Zhuang, Y.; Zeng, W.; Zhong, T. Measuring Daily Accessed Street Greenery: A Human-Scale Approach for Informing Better Urban Planning Practices. *Landsc. Urban Plan.* **2019**, *191*, 103434. [CrossRef]
6. Labib, S.M.; Lindley, S.; Huck, J.J. Spatial Dimensions of the Influence of Urban Green-Blue Spaces on Human Health: A Systematic Review. *Environ. Res.* **2020**, *180*, 108869. [CrossRef]
7. Zhou, H.; Liu, L.; Lan, M.; Zhu, W.; Song, G.; Jing, F.; Zhong, Y.; Su, Z.; Gu, X. Using Google Street View Imagery to Capture Micro Built Environment Characteristics in Drug Places, Compared with Street Robbery. *Comput. Environ. Urban Syst.* **2021**, *88*, 101631. [CrossRef]
8. Wang, R.; Liu, Y.; Lu, Y.; Zhang, J.; Liu, P.; Yao, Y.; Grekousis, G. Perceptions of Built Environment and Health Outcomes for Older Chinese in Beijing: A Big Data Approach with Street View Images and Deep Learning Technique. *Comput. Environ. Urban Syst.* **2019**, *78*, 101386. [CrossRef]
9. Bolte, A.-M.; Kötter, T.; Schuppe, S. Can You See Green or Blue? On the Necessity of Visibility Analysis of Urban Open Spaces Using Remote Sensing Techniques and Geographic Information Systems. In Proceedings of the 2019 Joint Urban Remote Sensing Event (JURSE), Vannes, France, 22 May 2019; pp. 1–4.
10. Fan, P.Y.; Chun, K.P.; Mijic, A.; Tan, M.L.; Liu, M.S.; Yetemen, O. A Framework to Evaluate the Accessibility, Visibility, and Intelligibility of Green-Blue Spaces (GBSs) Related to Pedestrian Movement. *Urban For. Urban Green.* **2022**, *69*, 127494. [CrossRef]
11. Rahman, M.S.; Meenar, M.; Labib, S.; Howell, T.; Adlakha, D.; Woodward, B. Unveiling Environmental Justice in Two US Cities through Greenspace Accessibility and Visible Greenness Exposure. *Urban For. Urban Green.* **2024**, *101*, 128493. [CrossRef]
12. Wu, C.; Du, Y.; Li, S.; Liu, P.; Ye, X. Does Visual Contact with Green Space Impact Housing Prices? An Integrated Approach of Machine Learning and Hedonic Modeling Based on the Perception of Green Space. *Land Use Policy* **2022**, *115*, 106048. [CrossRef]
13. Schmid, H.-L.; Säumel, I. Outlook and Insights: Perception of Residential Greenery in Multistorey Housing Estates in Berlin, Germany. *Urban For. Urban Green.* **2021**, *63*, 127231. [CrossRef]
14. Pristeri, G.; Peroni, F.; Pappalardo, S.E.; Codato, D.; Masi, A.; De Marchi, M. Whose Urban Green? Mapping and Classifying Public and Private Green Spaces in Padua for Spatial Planning Policies. *ISPRS Int. J. Geo-Inf.* **2021**, *10*, 538. [CrossRef]
15. Xiao, Y.; Li, Z.; Webster, C. Estimating the Mediating Effect of Privately-Supplied Green Space on the Relationship between Urban Public Green Space and Property Value: Evidence from Shanghai, China. *Land Use Policy* **2016**, *54*, 439–447. [CrossRef]

16. Coolen, H.; Meesters, J. Private and Public Green Spaces: Meaningful but Different Settings. *J. Hous. Built Environ.* **2012**, *27*, 49–67. [CrossRef]
17. Chen, Y.; Zhang, Q.; Deng, Z.; Fan, X.; Xu, Z.; Kang, X.; Pan, K.; Guo, Z. Research on Green View Index of Urban Roads Based on Street View Image Recognition: A Case Study of Changsha Downtown Areas. *Sustainability* **2022**, *14*, 16063. [CrossRef]
18. Mathieu, R.; Freeman, C.; Aryal, J. Mapping Private Gardens in Urban Areas Using Object-Oriented Techniques and Very High-Resolution Satellite Imagery. *Landsc. Urban Plan.* **2007**, *81*, 179–192. [CrossRef]
19. Kucherova, A.; Narvaez, H. Urban Forest Revolution. *E3S Web Conf.* **2018**, *33*, 01013. [CrossRef]
20. Haaland, C.; Van Den Bosch, C.K. Challenges and Strategies for Urban Green-Space Planning in Cities Undergoing Densification: A Review. *Urban For. Urban Green.* **2015**, *14*, 760–771. [CrossRef]
21. Šiftová, J. Shaping the Urban Home Garden: Socio-Ecological Forces in the Management of Private Green Spaces. *Land Use Policy* **2021**, *111*, 105784. [CrossRef]
22. Hua, J.; Cai, M.; Shi, Y.; Ren, C.; Xie, J.; Chung, L.C.H.; Lu, Y.; Chen, L.; Yu, Z.; Webster, C. Investigating Pedestrian-Level Greenery in Urban Forms in a High-Density City for Urban Planning. *Sustain. Cities Soc.* **2022**, *80*, 103755. [CrossRef]
23. Scheerlinck, K.; Schoonjans, Y. Garden Streetscapes: Front Yards as Territorial Confi Gurations. *Landsc. Rev.* **2016**, *16*, 43–58. [CrossRef]
24. Yang, J.; Zhao, L.; Mcbride, J.; Gong, P. Can You See Green? Assessing the Visibility of Urban Forests in Cities. *Landsc. Urban Plan.* **2009**, *91*, 97–104. [CrossRef]
25. Zhang, J.; Hu, A. Analyzing Green View Index and Green View Index Best Path Using Google Street View and Deep Learning. *J. Comput. Des. Eng.* **2022**, *9*, 2010–2023. [CrossRef]
26. Li, X.; Zhang, C.; Li, W.; Ricard, R.; Meng, Q.; Zhang, W. Assessing Street-Level Urban Greenery Using Google Street View and a Modified Green View Index. *Urban For. Urban Green.* **2015**, *14*, 675–685. [CrossRef]
27. Larkin, A.; Hystad, P. Evaluating Street View Exposure Measures of Visible Green Space for Health Research. *J. Expo. Sci. Environ. Epidemiol.* **2019**, *29*, 447–456. [CrossRef]
28. Helbich, M.; Yao, Y.; Liu, Y.; Zhang, J.; Liu, P.; Wang, R. Using Deep Learning to Examine Street View Green and Blue Spaces and Their Associations with Geriatric Depression in Beijing, China. *Environ. Int.* **2019**, *126*, 107–117. [CrossRef]
29. Ito, K.; Biljecki, F. Assessing Bikeability with Street View Imagery and Computer Vision. *Transp. Res. Part C Emerg. Technol.* **2021**, *132*, 103371. [CrossRef]
30. Shamseer, L.; Moher, D.; Clarke, M.; Ghersi, D.; Liberati, A.; Petticrew, M.; Shekelle, P.; Stewart, L.A. Preferred Reporting Items for Systematic Review and Meta-Analysis Protocols (PRISMA-P) 2015: Elaboration and Explanation. *BMJ* **2015**, *349*, g7647. [CrossRef]
31. Biljecki, F.; Ito, K. Street View Imagery in Urban Analytics and GIS: A Review. *Landsc. Urban Plan.* **2021**, *215*, 104217. [CrossRef]
32. Labib, S.M.; Huck, J.J.; Lindley, S. Modelling and Mapping Eye-Level Greenness Visibility Exposure Using Multi-Source Data at High Spatial Resolutions. *Sci. Total Environ.* **2021**, *755*, 143050. [CrossRef]
33. Yu, S.; Yu, B.; Song, W.; Wu, B.; Zhou, J.; Huang, Y.; Wu, J.; Zhao, F.; Mao, W. View-Based Greenery: A Three-Dimensional Assessment of City Buildings' Green Visibility Using Floor Green View Index. *Landsc. Urban Plan.* **2016**, *152*, 13–26. [CrossRef]
34. Long, Y.; Liu, L. How Green Are the Streets? An Analysis for Central Areas of Chinese Cities Using Tencent Street View. *PLoS ONE* **2017**, *12*, e0171110. [CrossRef] [PubMed]
35. Dong, R.; Zhang, Y.; Zhao, J. How Green Are the Streets Within the Sixth Ring Road of Beijing? An Analysis Based on Tencent Street View Pictures and the Green View Index. *Int. J. Environ. Res. Public Health* **2018**, *15*, 1367. [CrossRef]
36. Gong, F.-Y.; Zeng, Z.-C.; Zhang, F.; Li, X.; Ng, E.; Norford, L.K. Mapping Sky, Tree, and Building View Factors of Street Canyons in a High-Density Urban Environment. *Build. Environ.* **2018**, *134*, 155–167. [CrossRef]
37. Hu, T.; Wei, D.; Su, Y.; Wang, X.; Zhang, J.; Sun, X.; Liu, Y.; Guo, Q. Quantifying the Shape of Urban Street Trees and Evaluating Its Influence on Their Aesthetic Functions Based on Mobile Lidar Data. *ISPRS J. Photogramm. Remote Sens.* **2022**, *184*, 203–214. [CrossRef]
38. Seiferling, I.; Naik, N.; Ratti, C.; Proulx, R. Green Streets − Quantifying and Mapping Urban Trees with Street-Level Imagery and Computer Vision. *Landsc. Urban Plan.* **2017**, *165*, 93–101. [CrossRef]
39. Richards, D.R.; Edwards, P.J. Quantifying Street Tree Regulating Ecosystem Services Using Google Street View. *Ecol. Indic.* **2017**, *77*, 31–40. [CrossRef]
40. Zhang, Y.; Dong, R. Impacts of Street-Visible Greenery on Housing Prices: Evidence from a Hedonic Price Model and a Massive Street View Image Dataset in Beijing. *ISPRS Int. J. Geo-Inf.* **2018**, *7*, 104. [CrossRef]
41. Li, X. Examining the Spatial Distribution and Temporal Change of the Green View Index in New York City Using Google Street View Images and Deep Learning. *Environ. Plan. B Urban Anal. City Sci.* **2021**, *48*, 2039–2054. [CrossRef]
42. Wang, R.; Feng, Z.; Pearce, J.; Yao, Y.; Li, X.; Liu, Y. The Distribution of Greenspace Quantity and Quality and Their Association with Neighbourhood Socioeconomic Conditions in Guangzhou, China: A New Approach Using Deep Learning Method and Street View Images. *Sustain. Cities Soc.* **2021**, *66*, 102664. [CrossRef]
43. Lu, Y.; Yang, Y.; Sun, G.; Gou, Z. Associations between Overhead-View and Eye-Level Urban Greenness and Cycling Behaviors. *Cities* **2019**, *88*, 10–18. [CrossRef]
44. Lu, Y.; Sarkar, C.; Xiao, Y. The Effect of Street-Level Greenery on Walking Behavior: Evidence from Hong Kong. *Soc. Sci. Med.* **2018**, *208*, 41–49. [CrossRef] [PubMed]

45. Lu, Y. Using Google Street View to Investigate the Association between Street Greenery and Physical Activity. *Landsc. Urban Plan.* **2019**, *191*, 103435. [CrossRef]
46. Xiao, Y.; Miao, S.; Zhang, Y.; Xie, B.; Wu, W. Exploring the Associations between Neighborhood Greenness and Level of Physical Activity of Older Adults in Shanghai. *J. Transp. Health* **2022**, *24*, 101312. [CrossRef]
47. Ki, D.; Lee, S. Analyzing the Effects of Green View Index of Neighborhood Streets on Walking Time Using Google Street View and Deep Learning. *Landsc. Urban Plan.* **2021**, *205*, 103920. [CrossRef]
48. Huang, S.; Zhu, J.; Zhai, K.; Wang, Y.; Wei, H.; Xu, Z.; Gu, X. Do Emotional Perceptions of Visible Greeneries Rely on the Largeness of Green Space? A Verification in Nanchang, China. *Forests* **2022**, *13*, 1192. [CrossRef]
49. Kang, Y.; Zhang, F.; Gao, S.; Lin, H.; Liu, Y. A Review of Urban Physical Environment Sensing Using Street View Imagery in Public Health Studies. *Ann. GIS* **2020**, *26*, 261–275. [CrossRef]
50. Zhang, L.; Tan, P.Y.; Richards, D. Relative Importance of Quantitative and Qualitative Aspects of Urban Green Spaces in Promoting Health. *Landsc. Urban Plan.* **2021**, *213*, 104131. [CrossRef]
51. Helbich, M.; Poppe, R.; Oberski, D.; Zeylmans van Emmichoven, M.; Schram, R. Can't See the Wood for the Trees? An Assessment of Street View- and Satellite-Derived Greenness Measures in Relation to Mental Health. *Landsc. Urban Plan.* **2021**, *214*, 104181. [CrossRef]
52. He, N.; Li, G. Urban Neighbourhood Environment Assessment Based on Street View Image Processing: A Review of Research Trends. *Environ. Chall.* **2021**, *4*, 100090. [CrossRef]
53. Stancato, G. Integrated Analysis of Visual Change Points along Pathways: Automation and Comparison with Image Segmentation and Isovist Representation. In Proceedings of the ICGG 2024—Proceedings of the 21st International Conference on Geometry and Graphics; Takenouchi, K., Ed.; Springer Nature: Cham, Switzerland, 2024; pp. 256–267.
54. Comune di Milano Nuclei Di Identità Locale (NIL) | PGT. Available online: https://www.pgt.comune.milano.it/psschede-dei-nil-nuclei-di-identita-locale/nuclei-di-identita-locale-nil (accessed on 28 January 2024).
55. Anguelov, D.; Dulong, C.; Filip, D.; Frueh, C.; Lafon, S.; Lyon, R.; Ogale, A.; Vincent, L.; Weaver, J. Google Street View: Capturing the World at Street Level. *Computer* **2010**, *43*, 32–38. [CrossRef]
56. ADE20K Dataset. Available online: https://groups.csail.mit.edu/vision/datasets/ADE20K/ (accessed on 22 September 2023).
57. Huber, P.J. Robust Estimation of a Location Parameter. *Ann. Math. Stat.* **1964**, *35*, 73–101. [CrossRef]
58. Shapiro, S.S.; Wilk, M.B. An Analysis of Variance Test for Normality (Complete Samples). *Biometrika* **1965**, *52*, 591–611. [CrossRef]
59. Moran, P.A.P. Notes on Continuous Stochastic Phenomena. *Biometrika* **1950**, *37*, 17. [CrossRef]
60. Getis, A.; Aldstadt, J. Constructing the Spatial Weights Matrix Using a Local Statistic. *Geogr. Anal.* **2004**, *36*, 90–104. [CrossRef]
61. Cooke, A.; Smith, D.; Booth, A. Beyond PICO: The SPIDER Tool for Qualitative Evidence Synthesis. *Qual. Health Res.* **2012**, *22*, 1435–1443. [CrossRef]
62. Methley, A.M.; Campbell, S.; Chew-Graham, C.; McNally, R.; Cheraghi-Sohi, S. PICO, PICOS and SPIDER: A Comparison Study of Specificity and Sensitivity in Three Search Tools for Qualitative Systematic Reviews. *BMC Health Serv. Res.* **2014**, *14*, 579. [CrossRef]
63. Harzing, A.-W. *The Publish or Perish Book: Your Guide to Effective and Responsible Citation Analysis*, 1st ed.; Tarma Software Research Pty Ltd.: Melbourne, Australia, 2010; ISBN 978-0-9808485-0-2.
64. The Magpylib Documentation—Magpylib 4.4.0 Documentation. Available online: https://magpylib.readthedocs.io/en/latest/index.html (accessed on 22 September 2023).